Remarks

The format of the priority claim language was objected to. Further, claims 38-51 were rejected based on § 112, first paragraph (breadth of enablement), claims 39-42 and 49-50 were rejected based on § 112, second paragraph (omission between elements), claims 38, 51 and 52 were rejected based on § 112, second paragraph (indefiniteness), and claim 52 was rejected based on § 101 (subject matter). In view of the amendment above, the remarks below, and the enclosed submissions, reconsideration is respectfully requested.

Extension Petition

An extension petition is enclosed, together with a fee authorization. Hence, this amendment is timely since it is being filed prior to January 22, 2004.

§ 101

Claim 52 has been canceled, rendering the only § 101 rejection moot.

§ 112, First Paragraph - Enablement

The Office Action acknowledged that the application is enabling for at least some claimed embodiments. However, it asserted that the claims were not sufficiently enabled given the breadth of the claims. This latter finding is respectfully traversed to the extent it would be applied against the above set of amended claims.

The central teaching of the present application, regarding the _ability_ of a polypeptide to form fibrils, _is_ broadly applicable to polypeptides. Of course, the propensity to do so will vary based on the specific conditions. However, enablement should not be confused with optimization.

Prior to the present invention there were a variety of teachings of ways to manipulate the conditions of incubation of a protein, for example changes that result in protein denaturation. However, before the present application there was no appreciation in the art that proteins could be made to

6

form amyloid fibrils by altering conditions, or generally what types of alterations would achieve this.

Thus, before the present application, the skilled artisan would have had no motivation to attempt to form amyloid fibrils from any protein as he/she would not have appreciated that this would even be possible. The artisan would therefore not have considered applying the artisan's knowledge of varying conditions such as pH, temperature and solutes in order to form amyloid fibrils.

However, with the teachings of the present application, that situation has changed. While specific optimal conditions required to cause fibril formation will vary somewhat for different proteins, as evidenced by the experimental examples of the present application where slightly different conditions are preferred for different proteins, once the skilled artisan learns of the possibility of creating them, and the basic approaches of how to do so from the present application, it would be a matter of routine experimentation to achieve at least some aggregation and fibril formation for still other types of proteins. Crude aggregation and fibril formation should quickly be achieved (which is all that is needed for enablement), and even optimization should be relatively easy to achieve.

The skilled artisan would readily understand (on the basis of the present application in combination with his/her general knowledge of the field and the particular protein selected) what modifications should be made for different proteins. Such modifications can be carried out in a systematic way by the skilled artisan by varying, for example, the concentration of protein, the pH, the temperature, the type and amount of co-solvent, the ionic strength of the solution, or by introducing mutations of residues to increase amyloidogenicity. These variations would be straightforward to carry out.

The application itself exemplifies using a variety of proteins. For example, Examples 1 and 2 show that at acid pH, P13-SH3, a small globular domain with a simple native fold, aggregates readily into amyloid fibrils. At neutral pH, this domain, which folds without accumulation of intermediates, does not form amyloid deposits. See J. Guijarro et al., 95 PNAS USA 4224-4228 (1998), already of record. These results suggest to one skilled in the art that at acid pH, an amyloid favoring conformation, not accessible at neutral pH, is populated.

This conformational state is a conformational mixture of partially folded molecules, which will contain a dynamic distribution of structures, some of which will be highly unfolded and others of which will be highly compact. In the case of previously known amyloidogenic proteins such as transthyretin, lysozyme and the Ig light chain, partly folded states in equilibrium with the native protein are known to be populated under conditions favoring amyloid formation. The data in the present application and the Guijarro paper indicates that partially folded states, whether in equilibrium with unfolded or native proteins, are precursors to the formation of amyloid fibrils.

Similarly, as shown in Example 3 (and in the enclosed paper M. Groß et al., 8 Protein Science 1350-1357 (1999)), characterization of the aggregated CspB proteins by circular dichroism and NMR spectroscopy shows that the formation of amyloid fibrils does not require any specific preformed secondary structure in the solution state protein. Structures including monomeric and unstructured proteins, α-helical, β-sheet and random coil conformations are observed under the conditions that eventually lead to fibril formation.

The present application itself thus demonstrates that a variety of protein types are capable of forming amyloid fibrils and no amyloid-associated disease of the proteins have

8

been identified. The results of the present application therefore demonstrate that such amyloid formation is a common property of proteins (under appropriate conditions) and that it is not a rare, exclusive property of a few proteins that are disease associated.

This is further supported by a substantial number of experimental results achieved after the present invention. We enclose papers published after the present invention where the teaching of the application has been used to generate amyloid fibrils from a variety of other polypeptides. The teaching of the application that fibril formation is a generic property of polypeptides, rather than specific to a narrow subset of proteins, is therefore strongly supported by the subsequent research in this field.

For example, although amyloid fibrils are characteristically rich in β-sheets, amyloid fibrils can be formed from proteins which lack β-sheet structure, such as α-helical proteins. The documents enclosed include examples of amyloid fibril formation from helical proteins such as the archetypal soluble protein myoglobin (M. Fändrich et al., 410 Nature 165-166 (2001) and type 1 antifreeze protein from winter flounder (S. Graether et al., 84 Biophysical Journal 552-557 (2003).

M. Fändrich et al., 21 J. EMBO 5682-5690 (2002), a copy of which is enclosed, demonstrates amyloid fibril formation from homopolymeric amino acids such as polythreonine and polylysine. This shows that, unlike in normal protein folding, specific sequence patterns are unnecessary for the ability to form fibrils. Rather, the formation of amyloid fibrils appears to be a result of the formation of aberrant protein conformations.

The Office Action suggested that the presence of "an alcohol and acetonitrile or urea" may be an essential feature of the invention and (apart from the protein types) should be

9

included in the claims. The Applicant respectfully submits that this is not the case.

A denaturing step, for example the addition of an alcohol, acetonitrile or urea to the protein, is only required for processes involving globular proteins. See page 4, lines 25-30 and page 5, lines 4-8, regarding denaturation procedures via a variety of ways, all of which have the same ultimate effect. Fibrils can generally be formed from globular proteins by placing them under mildly denaturing conditions. While newly submitted dependent claims 54 and 55 have therefore been added directed to these embodiments in view of the Office's favorable finding with respect thereto, claim 38 has not been amended to include it because the invention is not limited to just globular proteins.

Where amyloid fibrils are formed from non-globular proteins such as peptides and unstructured proteins by placing them under conditions of pH and ionic strength, etc. to generate the appropriate conditions for fibril formation, newly submitted dependent claim 59 would be more pertinent.

Similarly, contrary to the Office Action's preliminary finding, it is believed that the claims are more broadly enabled than just the claim 50 copper, silver and gold subject matter. For example, as the amyloid fibrils form, they may be covalently linked to a variety of metal particles. This forms peptide "nanotubes" that may improve, for example, the strength and/or electrical conductivity of the amyloid fibrils. The metal is thus incorporated into the structure of the amyloid fibrils when they form. There is no reason why this aspect should be limited to the use of copper, silver and gold. The skilled person would appreciate on the basis of the application, and his knowledge of the art, that the same principles can be applied to other types of materials.

The Office Action refers to a paper by Perutz et al. However, this paper merely speculates about various

structures, and runs no experiments following Applicant's teachings to try to form the fibers.

Further, Perutz states at page 5594 column 2 that it is "difficult to guess" what structure naturally occurring full-length huntingtin fibers may have. Perutz goes on to hypothesize about what that structure may be. Even Perutz's "teaching" that amyloids consist of narrow tubes with a central water-filled cavity (page 5595, column 1) is preceded by the proviso "if this interpretation is correct". The purported "teaching" of Perutz would not in any event mandate the inapplicability of Applicant's teaching.

Hence, Perutz does not demonstrate that any particular protein cannot be made to form fibrils using the teaching of the present invention. Indeed, any adverse interpretation of Perutz would be inconsistent with the actual experimental results of M. Fändrich et al. (2002) and Fändrich et al. (2001) (both enclosed), which suggest that neither the amino acid sequence, nor the secondary structure of a protein, is critical to its ability to form amyloid fibrils.

Further, the Office Action's reliance on F. Chiti et al., 96 PNAS USA 3590-3594 (1999) for support is misplaced. The last named author of that article is the named inventor of the present application. Inventor Dobson is familiar with the article as well as the intent of the statements therein.

The cited sentence in the Office Action was intended merely as an indication that optimal conditions would vary based on the proteins selected, not that they had reason to believe that the invention couldn't apply at least to some extent to a known subset of proteins. This is confirmed by the following two sentences:

> ...As with the formation of crystals, the
> conditions for optimum growth are likely
> to be highly dependent on the properties
> of the particular system under study. We
> believe, however, that conditions that
> will generally give rise to efficient

11

> formation of amyloid will be partially
> denaturing and will be such as to allow
> the slow and controlled growth of
> aggregated species. [emphasis added]

Hence, the cited sentence was merely intended to indicate that "optimum" conditions would vary, not that crude formation would not occur. Further, the last sentence noted above indicates that the procedures for formation followed generally similar principles.

Hence, the abstract of the Chiti et al. article ends with the statement:

> ...We suggest that amyloid formation
> is not restricted to a small number of
> protein sequences but is a property common
> to many, if not all, natural polypeptide
> chains...

As such, far from questioning scope of enablement, this article confirms breadth of enablement.

Of course, Patent Office policy has never required an applicant to submit experimental evidence of every possible specie within a claim being enabled. All that is required are representative indications of a broad enablement. Here, several representative examples are provided in the application itself. Also, the enclosed additional art confirms further breadth of the enabling nature of the invention. Not a single example has been cited by the Office of the art finding that Applicant's approach does not work when tried.

As such, Applicant respectfully submits that the claims should now be deemed adequately enabled.

§ 112, Second Paragraph - Omission Of Elements

Applicant is not sure as to the rationale behind the Office's objection regarding claims 39-42 and 49-50 with respect to the "omission" of the concentrations of these additives, or how or why that would constitute a concern under

§ 112, second paragraph. Each of these claims merely adds an additional limitation to claim 38.

The claims, due to the way they are written, presently indicate a percentage greater than zero and less than 100% (the latter because there must also be protein). While that is not a narrow range, it is <u>not</u> an indefinite range.

The fact that Applicant could have written those claims with molarity or weight percentage limitations to cover a narrower range of embodiments does not affect the clarity of the claims as they now are. Breadth should not be confused with definiteness.

Without prejudice to Applicant's arguments, newly submitted claims 56-58 are presented with more focus on such limitations, and new claim 60 presents a preferred set of conditions in independent form.

§ 112 – Second Paragraph – Indefiniteness

Claim 38 has been amended to remove the term "over an acceptable time". This renders the claim 38 rejection for indefiniteness moot.

Claims 51 and 52 are now cancelled without prejudice. Hence, the indefiniteness rejections relating thereto are now also moot.

Conclusion

In view of the above amendment and remarks, and the enclosed submission, reconsideration and allowance are respectfully requested with respect to amended claims 38-50, and newly submitted claims 54-60. The claims pending after amendment are still no greater than twenty in number, and the independent claims pending after amendment are only two. Hence, no additional fee is believed needed to pay for the additional claims to be considered.

As such, no additional fees, apart from the three month extension fee, are believed to be needed for the submission,

entry and full consideration of this amendment. However, if
any are, please charge them to Deposit Account 17-0055.

Respectfully submitted,

Christopher M. Dobson

Dated: January 13, 2004   By:_____

Carl R. Schwartz, Esq.
Reg. No.: 29,437
Quarles & Brady LLP
411 East Wisconsin Avenue
Milwaukee, Wisconsin 53202
(414) 277-5715

MKE\5518926.1

14

Formation of amyloid fibrils by peptides derived from the bacterial cold shock protein CspB

MICHAEL GROß,[1] DEBORAH K. WILKINS,[1] MAUREEN C. PITKEATHLY,[1]
EVONNE W. CHUNG,[1] CLAIRE HIGHAM,[2] ANNE CLARK,[2] AND CHRISTOPHER M. DOBSON[1]

[1]Oxford Centre for Molecular Sciences, University of Oxford, New Chemistry Laboratory, Oxford OX1 3QT, United Kingdom
[2]Department of Human Anatomy, University of Oxford, South Parks Road, Oxford OX1 3QT, United Kingdom

Abstract

Three peptides covering the sequence regions corresponding to the first two (CspB-1), the first three (CspB-2), and the last two (CspB-3) β-strands of CspB, the major cold shock protein of *Bacillus subtilis*, have been synthesized and analyzed for their conformations in solution and for their precipitation behavior. The peptides are nearly insoluble in water, but highly soluble in aqueous solutions containing 50% acetonitrile (pH 4.0). Upon shifts of the solvent condition toward lower or higher acetonitrile concentrations, the peptides all form fibrils resembling those observed in amyloid associated diseases. These fibrils have been identified and characterized by electron microscopy, binding of the dye congo red, and X-ray fiber diffraction. Characterization of the peptides in solution by circular dichroism and NMR spectroscopy shows that the formation of these fibrils does not require specific preformed secondary structure in the solution state species. While the majority of the soluble fraction of each peptide is monomeric and unstructured, different types of structures including α-helical, β-sheet, and random coil conformations are observed under conditions that eventually lead to fibril formation. We conclude that the absence of tertiary contacts under solution conditions where binding interactions between peptide units are still favorable is a crucial requirement for amyloid formation. Thus, fragmentation of a sequence, like partial chemical denaturation or mutation, can enhance the capacity of specific protein sequences to form such fibrils.

Keywords: acetonitrile; aggregation; amyloid; β-sheet; circular dichroism; electron microscopy; misfolding; NMR spectroscopy

Proteins forming fibrillar aggregates have been shown to be associated with a wide range of medical conditions, including the prion diseases (Harrison et al., 1997), Alzheimer's disease (Beyreuther & Masters, 1997), familial amyloid polyneuropathy (Kelly, 1997), and type II diabetes (Westermark et al., 1987). Current structural models suggest that the main molecular features of these amyloid fibrils involve β-sheets organized as extended cross β structures with a helical twist (Blake & Serpell, 1996; Sunde & Blake, 1997), as a β-helix with between 9 and 24 residues per turn (Lazo & Downing, 1998), or as short, nontwisted β-sheets linked by loops

(Jiménez et al., 1999). The mechanism of the formation of such proteinaceous fibrils is not known in molecular detail, although general models for specific cases have been proposed (Arvinte et al., 1993). The origin of amyloid deposit is also not well established. A sequence determinant, which makes a protein or peptide potentially amyloidogenic, has been proposed (Kurochkin, 1998), but the growing number of unrelated proteins forming fibrils closely similar to those found in amyloid deposits associated with chronical diseases suggests the propensity for this structure is inherent in the polypeptide backbone (Guijarro et al., 1998; Chiti et al., 1999). In this paper, all such fibrils will be called "amyloid fibrils" if they give the characteristic results in electron microscopy, congo red binding, and birefringence of congo red stained fibrils, whether or not they derive from pathogenic processes. A thorough understanding of the mechanisms and driving forces leading to amyloid fibril formation is required for the identification of novel strategies to prevent or cure the diseases with which they are associated.

In the context of a research project aimed at the folding of nascent protein chains (Groß, 1996; Groß & Dobson, 1997), we have investigated the solution properties of three synthetic pep-

tides derived from the cold shock protein CspB from *Bacillus subtilis*. CspB has been shown by X-ray crystallography (Schindelin et al., 1993) as well as by NMR (Schnuchel et al., 1993) to have a simple all β-sheet topology homologous to the S1 domain (Bycroft et al., 1997). Like S1 and the homologous *Escherichia coli* cold shock protein, CspA, the *Bacillus* protein has been shown to bind single-stranded RNA, and it is thought to act as an RNA chaperone in that it stops mRNA from forming unwanted secondary structure at low temperatures (Graumann & Marahiel, 1997; Graumann & Marahiel, 1998). CspB is remarkable for its ability to fold very rapidly (Schindler et al., 1995; Schindler & Schmid, 1996), and for its relatively low contact order (Plaxco et al., 1998) (i.e., a high proportion of contacts between residues close to each other in the linear sequence). As all the β-sheet forming interactions occur between strands that are neighboring in the sequence, secondary structure formation might be possible both during the synthesis on the ribosome and also within the short peptide fragments investigated here.

Although this protein is not related to any of the at least 18 known eukaryotic constituents of pathological amyloid fibrils (Sunde & Blake, 1997), we find that all three peptides in our study precipitate as fibrils with characteristics closely similar to mammalian amyloid from a variety of conditions where highly unstructured monomers are the prevailing species in solution. It follows that the initial secondary structure content of the monomeric polypeptide is not a major determinant of amyloid formation. The most important requirement appears to be the lack of ordered tertiary structure under conditions where interactions such as hydrogen bonds or hydrophobic contacts are still viable (Chiti et al., 1999). This requirement can be met either by conditions that induce at least partial unfolding of the intact protein, or by dissecting a polypeptide chain into shorter peptides that are unable to form cooperative globular structure, as we demonstrate in this paper. Here we present results that characterize both the fibrils and the solution state from which they arise.

Results and discussion

Based on the known structure of the *B. subtilis* cold shock protein CspB, consisting of five β-strands arranged in a small β sandwich (Schindelin et al., 1993; Schnuchel et al., 1993), the peptides CspB-1 (residues 1–22), CspB-2 (1–35), and CspB-3 (36–67) were designed to correspond to the first two, the first three, and the last two β-strands of the protein, respectively (Fig. 1). While CspB-1 and CspB-2 mimic a nascent protein growing from the N-terminus, CspB-2 and CspB-3 represent the two halves of the β sandwich and together cover the entire sequence length of the original protein.

Cold shock protein B is soluble in aqueous buffers at pH values ranging from 6.0 to 7.2 to a protein concentration of at least 1.3 mM (10 mg/mL), as demonstrated by the fact that the NMR structure was obtained under these conditions (Schnuchel et al., 1993). In contrast, neither of the three peptides investigated here is soluble under similar conditions to any significant extent; CspB-2, for example, dissolves only to ~0.2 mg/mL. To solubilize the peptides, we used acetonitrile as a cosolvent at pH 4.0 (formic acid, unbuffered). All three peptides are soluble to 10 mg/mL or higher under these conditions, although their solubility decreases drastically if the acetonitrile concentration is changed to values significantly higher or lower than 50%. For example, attempts to prepare NMR samples by diluting stock solutions containing 20
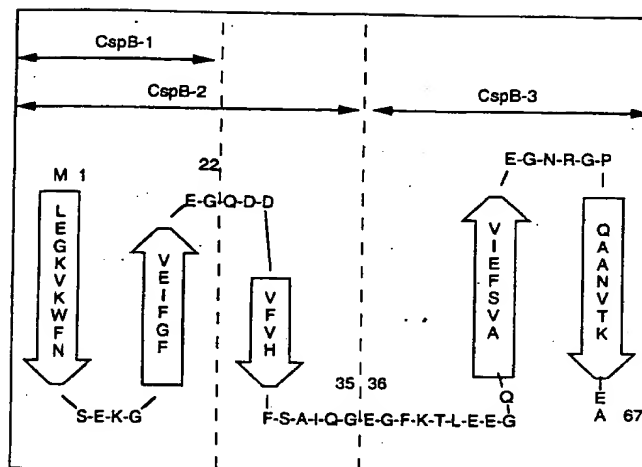

Fig. 1. Sequence and secondary structure content of the cold shock protein CspB from *Bacillus subtilis*. The numbers indicate the first and last amino acids of the three peptides used in this study: CspB-1 (1–22), CspB-2 (1–35), and CspB-3 (36–67).

mg/mL peptide in 50% acetonitrile with four volumes of either water or acetonitrile resulted in rapid precipitation of the peptides. A standardized set of combinations of peptide concentration and solvent composition was used in the experiments described here, involving peptide concentrations of 0.4, 2, and 10 mg/mL, and acetonitrile concentrations of 10, 50, and 90%.

NMR studies of the three peptides were carried out under the conditions where they are most soluble (10 mg/mL peptide in 50% acetonitrile pH 4.0). CD studies were carried out at acetonitrile concentrations ranging from 5 to 95%. Due to the lower peptide concentrations needed for CD spectroscopy (0.4 mg/mL), spectra could still be obtained under conditions of relatively low solubility (i.e., in higher and lower concentrations of acetonitrile). The insoluble material produced by solvent shifts was analyzed by a variety of techniques including specific tests for the presence of amyloid fibrils.

CD measurements

The three peptides were found to differ substantially in their structural properties, as monitored by CD spectroscopy, particularly under the conditions where they are relatively insoluble and from which fibril formation can be initiated (see below). In the soluble state (50% acetonitrile), CspB-1 appears to be largely unstructured at 0.4 mg/mL (Fig. 2A,D), although it forms β-sheet structure at very high peptide concentrations, as indicated by additional CD measurements using a 0.1 mm pathlength cell. The ellipticity per residue increases from −1,730 to −6,480 deg cm²/dmol as the acetonitrile concentration is increased to 90%, suggesting ~70% of β structure at the highest acetonitrile concentration.

CspB-2 (Fig. 2B,D) adopts a largely β-sheet conformation at very high and at very low acetonitrile concentrations (100% β-sheet at 2.5% acetonitrile, and 71.5% β-sheet at 97.5% acetonitrile). It is less structured at intermediate solvent conditions (mean residue ellipticities around −3,410 deg cm²/dmol, indicating ~20% β-sheet content in the range from 15 to 70% acetonitrile). CspB-3
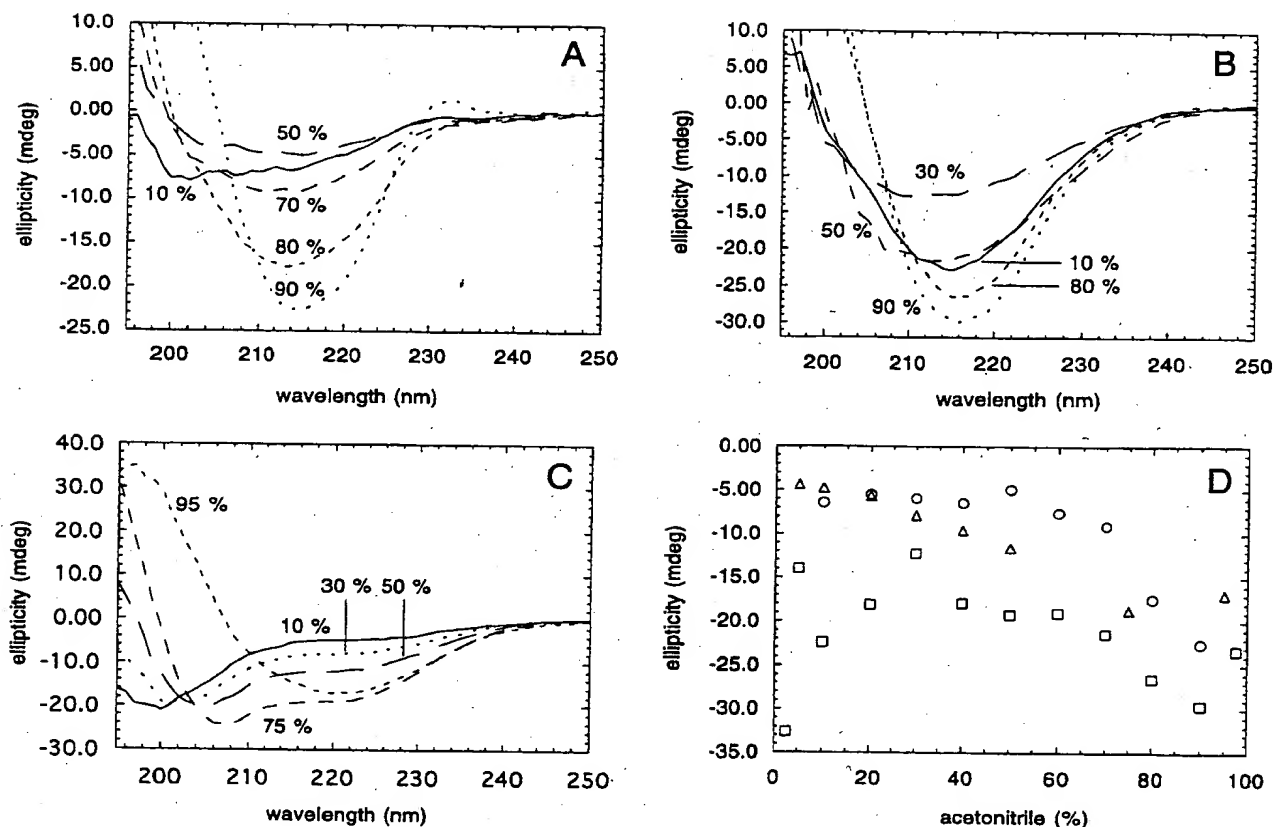
Fig. 2. Characterization of dilute solutions of the peptides by CD spectroscopy. Acetonitrile concentration was varied as indicated. A–C: CD spectra recorded at acetonitrile concentrations ranging from 2.5 to 97.5% of solutions containing 0.4 mg/mL of (A) CspB-1, (B) CspB-2, and (C) CspB-3. D: Ellipticity at 215 nm plotted against the acetonitrile concentration. Circles: CspB-1; squares: CspB-2; triangles: CspB-3.

(Fig. 2C,D) displays particularly interesting behavior as it can be in predominantly unstructured, partly helical, or largely β-sheet conformations depending on the acetonitrile concentration. The CD data show that the helix content increases gradually as the acetonitrile concentration is increased from 5 to 75%, but the peptide converts to predominant β-sheet structure at acetonitrile concentrations between 75 and 95%. At the latter concentration, the ellipticity per residue observed at 215 nM for this peptide is −3,830 deg cm²/dmol, corresponding to 41% β-sheet.

At low concentrations of acetonitrile (10%), CspB-2 adopts a β-sheet conformation, while the other two peptides are predominantly unstructured. At high acetonitrile concentrations (90%), however, all peptides show some extent of β-sheet formation, which overlaps with random coil properties for the two N-terminal peptides, and with α-helical structure for the C-terminal peptide (Fig. 2). CspB-3 changes sequentially from unstructured to helical to β-sheet conformation when gradually transferred from 5 to 95% acetonitrile. Generally, therefore, the β-sheet content increases when the conditions change toward lower solubility or higher acetonitrile concentration. This is indicative of intermolecular rather than intramolecular β-sheet formation. The data suggest that the monomers are mostly unstructured (or partially helical in the case of CspB-3), while the aggregates all contain β structure.

NMR experiments

NMR diffusion measurements (Jones et al., 1997) conducted at a peptide concentration of 10 mg/mL in 50% acetonitrile indicate a single diffusion constant for each peptide, corresponding to values of hydrodynamic radii similar to those predicted for unfolded monomers (Table 1). This suggests that the samples consist predominantly of monomers. Any small oligomers (whose signals merge with the monomer signal if conformational interconversion takes place on a time scale shorter than that resolvable by this method, i.e., less than ~100 ms) can only exist as minor populations. Calibration of the spectral intensities, however, indicates that these are lower than expected for the concentration of peptide involved. This was examined quantitatively for CspB-1, where it was found that only ~20% of the total peptide concentration present in the sample is detectable in the NMR spectra. The remainder must therefore be in large soluble aggregates whose overall tumbling times are too large to give resolvable NMR resonances.

Detailed structural NMR studies of all three peptides were undertaken at 20 and at 35 °C in solutions containing 50% acetonitrile. For all peptides, complete assignment of the amide resonances was achieved by analysis of COSY and TOCSY spectra acquired

Table 1. *Hydrodynamic radii[a] of CspB peptides at 10 mg/mL concentration in 50% acetonitrile, as determined by NMR diffusion measurements*

Peptide (no. of residues)	Hydrodynamic (Stokes) radius (nm)[b]	Predicted value for unfolded monomer (nm)[c]	Predicted value for unfolded dimer (nm)
CspB-1 (22)	1.60[a]	1.29	1.80
CspB-2 (35)	1.68	1.72	2.54
CspB-3 (32)	1.66	1.63	2.43

[a] Hydrodynamic radii were calculated using Stokes' law from diffusion measurements as described previously (Jones et al., 1997). The Stokes radius of CspB-1 was also determined in the supernatant of a sample containing 2 mg/mL peptide in 10% acetonitrile after fibril formation was completed. The Stokes radius of this species was 1.34 nm.

[b] HPLC analysis confirms that the peptides in their soluble states are largely monomeric, but provides evidence for minor populations of small oligomers. In chromatographic profiles, monomers are the dominant species, while dimers and higher order oligomers are present only at lower concentrations (<30%).

[c] Predictions are based on a fit of the hydrodynamic radii measured by pulse field gradient NMR for highly unfolded proteins and peptides, resulting in the empirical equation $R = 0.225N^{0.57}$ where R is the hydrodynamic radius in nm and N is the number of amino acid residues (D.K. Wilkins, J.A. Jones, V. Receveur, S.B. Grimshaw, L.J. Smith, C.M. Dobson, unpubl. results).

at 35 °C. None of the peptides showed any measurable long range NOEs or ROEs. This indicates the absence of any significant persistent structure. The structural characteristics of the peptides were therefore inferred by comparing their chemical shifts and coupling constants with those predicted from random coil models (Serrano, 1995; Smith et al., 1996). Although random coil values of chemical shifts are well documented (Wishart et al., 1995; Plaxco et al., 1997), the values obtained for amide protons are highly dependent on solvent conditions. Therefore, we used only the C_α proton shifts in this analysis. These show only minor deviations from typical random coil values (most between ±0.1, and all between −0.20 and +0.15 ppm).

Most of the coupling constants measured for CspB-1 are slightly larger than the values predicted for a random coil (Smith et al., 1996) (Fig. 3A). This indicates that CspB-1 has a slightly higher occupancy of the β-region of $\phi\psi$ space than anticipated for a random coil. This is most pronounced in the regions of residues 5–9 and 17–20 (Fig. 3A). Both these groups of residues are within the regions of the β-strands in the native protein (2–10, 15–20). For CspB-3, the coupling constant measurements show smaller values than predicted for a random coil, suggesting that the small amount of helical structure observed in the CD spectra is likely to be localized between residues 38 and 53 (Fig. 3B). This result is also in accord with the slight propensity for helix formation in this region revealed by several of the secondary structure prediction methods used. Thus, the Gibrat (Gibrat et al., 1987), Levin (Levin et al., 1986), DPM (Deleage & Roux, 1987), and SOPMA (Geourjon & Deleage, 1995) methods predict the conformation of the majority of the residues in positions 38 to 47 to be helical (data not shown). Additional helicity, which is predicted to occur near the carboxy terminus, was not observed by NMR.

Evidence for amyloid fibril formation

Analysis by three independent techniques of samples produced by dilution of concentrated solutions of all three peptides (10.0 mg/mL diluted to 2.0 mg/mL final concentration) from 50% to either 10 or 90% acetonitrile was carried out to screen for the presence of amyloid fibrils. CspB-1 was used for all further investigations into fibril formation. Spectroscopic binding assays using the diazo dye congo red (Fig. 4A) show the typical red shift in wavelength and increase in intensity characteristic of amyloid fibrils. In transmission electron microscopy (Fig. 4B), a dense network of straight and unbranched fibrils approximately 10 nm in diameter and up to 300 nm long was observed for CspB-1 diluted into 10% acetonitrile. Under other experimental conditions, and with the other peptides, fewer fibrils were observed, but similar morphologies were evident. Light microscopy of congo red stained precipitates using crossed polarizers (not shown) revealed the green birefringence characteristic of amyloid fibrils (Cooper, 1974).

Aggregated states of all three peptides produced in 10 and 90% acetonitrile were analyzed using these techniques. While all types of experiment were strongly positive for the presence of amyloid for CspB-1 in 10% acetonitrile, more varied results were obtained under some of the other conditions. Nevertheless, under all conditions positive evidence indicating formation of amyloid fibrils was obtained (Table 2).

Further examination was carried out with the fibrils formed by CspB-1 in 10% acetonitrile. Intermolecular β-sheet structure, which is compatible with fibril formation, was also demonstrated by FTIR (D.K. Wilkins, M. Groß, & C.M. Dobson, unpubl. results) for peptide CspB-1. X-ray fiber diffraction also yielded results characteristic of amyloid fibrils. For the latter technique, a sample of CspB-1 in 50% acetonitrile was left to dry down after suspending between two capillaries. As a result of the higher volatility of acetonitrile, the solvent composition changes during the evaporation and is expected to be near 10% acetonitrile during the actual precipitation process. This resulted in a thin needle of precipitate, which showed X-ray diffraction patterns (Fig. 4C,D) with diffraction maxima at 0.47 and 1.04 nm, typical of amyloid fibrils (Sunde & Blake, 1997).

Conclusions

We have shown that three peptides derived from a small bacterial protein with an all β structure can form amyloid fibrils, although there is no known link to a pathogenic amyloid forming protein. The formation of these fibrils can occur from quite different starting situations by solvent shifts toward higher or lower concentrations of acetonitrile. Typically, the solutions contain populations of largely unstructured monomers, together with oligomers and soluble aggregates containing significant amounts of β-sheet structure. This suggests that amyloid formation does not depend on the presence of extensive preformed secondary structure elements within monomeric species in solution, although the aggregates and the amyloid fibrils themselves contain extensive β-sheet structure. More generally, β structure is common within a wide range of aggregates of different morphologies (Fink, 1998). The ability to form aggregates with such β structure is likely to be an important factor in the subsequent conversion to ordered amyloid fibrils.

As far as the primary structure is concerned, a sequence motif, which is recognized by the insulin degrading enzyme (IDE), has recently been suggested to be a determinant for the formation of amyloid fibrils (Kurochkin, 1998). However, no such motif is
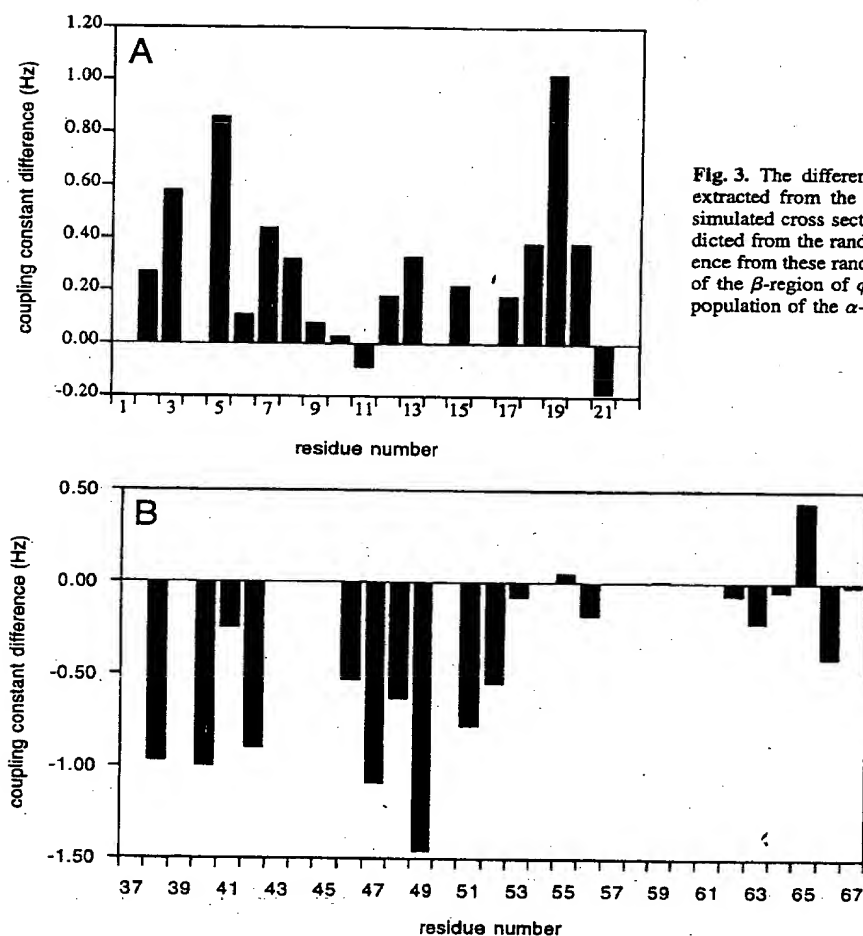
Fig. 3. The difference of the residue specific $^3J_{NH\alpha}$ coupling constants extracted from the antiphase splitting in a COSY spectra by fitting to . simulated cross sections for (A) CspB-1 and (B) CspB-3 from those predicted from the random coil model (Smith et al., 1996). A positive difference from these random coil values indicates an increase in the population of the β-region of $\phi\psi$ space, and negative differences an increase in the population of the α-region.

present in any of the three peptides studied here. Similarly, the SH3 domain from bovine phosphatidyl inositol 3-kinase, an 84 residue protein with five β-strands, which readily forms amyloid fibrils at acidic pH (Guijarro et al., 1998), does not contain such a motif. One protofilament structure proposed recently (Lazo & Downing, 1998) requires short β-strands with hydrophobic residues in every other position. Such sequence elements are indeed found in all of the CspB peptides studied here (e.g., residues 5–9, 47–51 in CspB, see Fig. 1), and in the sequence of the PI3–SH3 domain (e.g., residues 23–29: DIDLHLG). While the sequences matching this criterion provide some support for such a structural model, this sequence motif is not specific enough to draw strong conclusions from it.

It has been suggested that the formation of the characteristic cross β structure of the amyloid fibrils, in which the β-strands are oriented perpendicular to the fiber axis, reflects a natural bias of the polypeptide chain (Sunde & Blake, 1997). That this is not normally observed in biological systems is likely to arise predominantly from the cooperative formation of specific tertiary interactions characteristic of native globular proteins (Chiti et al., 1999). In denaturing conditions and in short peptides, therefore, the absence of specific tertiary interactions allows intermolecular interactions, which can ultimately lead to the formation of fibrillar structures.

The tertiary structure of a protein can be destabilized by partial denaturation, by mutation, or by dissection into short fragments.

For example, the SH3 domain was shown to form amyloid fibrils from a partially folded low pH state (Guijarro et al., 1998), a fibronectin module behaves similarly when heated (Litvinovich et al., 1998), as does acylphosphatase when it is dissolved in trifluoroethanol (TFE) at concentrations just sufficient to denature the protein (Chiti et al., 1999). In human lysozyme, a single destabilizing point mutation is sufficient to turn a normally stable monomeric protein into an amyloidogenic variant (Pepys et al., 1993; Booth et al., 1997). Moreover, short peptides derived from the amyloidogenic proteins transthyretin (Serpell, 1995), prions (Pillot et al., 1997), or Alzheimer-associated proteins (Han et al., 1995) can have stronger propensities to form amyloid fibrils than the full length proteins.

Here we have demonstrated therefore that peptides derived from a soluble globular protein not related to any pathogenic sequences can form amyloid fibrils. This reinforces the view that amyloid formation is a generic property of polypeptide chains, and that destabilization of tertiary structure is a major requirement for the formation of such aggregates. The latter suggests that agents enhancing the tertiary structure without increasing the secondary structure propensities of proteins could be useful as inhibitors of the pathological process of amyloidosis (Peterson et al., 1998). On the other hand, agents that favor secondary over tertiary structure may promote the growth of amyloid fibrils, as demonstrated by the
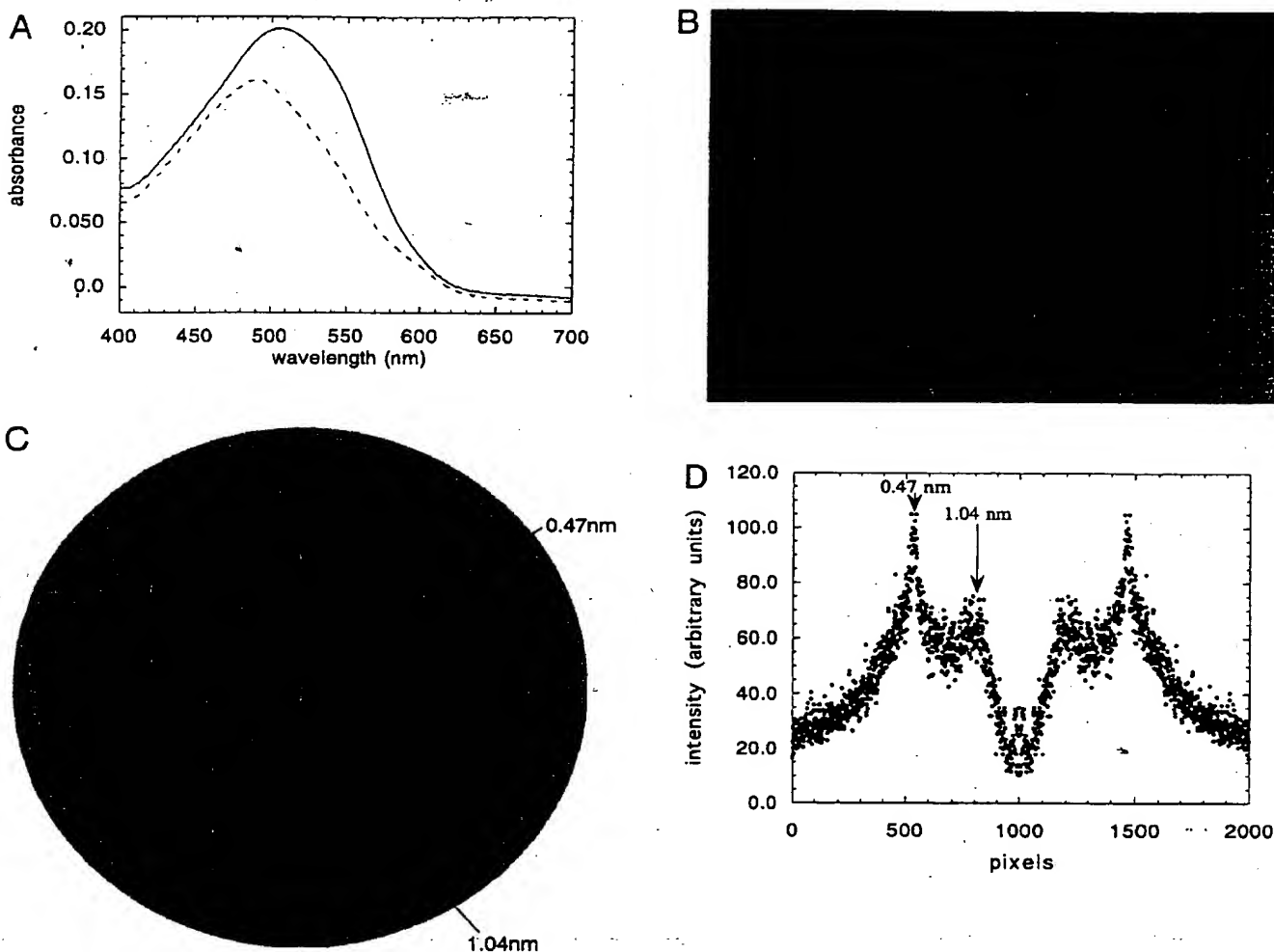
Fig. 4. Evidence for amyloid fibrils formed by CspB-1 upon reduction of the acetonitrile concentration. **A:** Example of the visible spectra of the congo red assay. The dashed line represents the spectrum before, the solid line the one after, addition of a sample of CspB-1 in 10% acetonitrile. The shift toward higher wavelengths and greater intensity indicates fibril formation. **B:** Electron micrograph of negatively stained fibrils. The scale bar corresponds to a length of 200 nm. **C:** X-ray fiber diffraction pattern obtained from a sample dried down from a 5 mg/mL solution in 50% acetonitrile. **D:** Cross section of the diffraction pattern in C with assignment of the peaks corresponding to the distances typical for β-sheet structure.

effect of TFE on acylphosphatase (Chiti et al., 1999). It is difficult to determine the localized conditions that affect misfolding events at the site of amyloid formation in vivo. Understanding the molecular details of the events giving rise to amyloid formation is, however, an important step in the quest to develop diagnostic and therapeutic agents for amyloid-related diseases. Given that amyloid fibril formation can be easily triggered in the peptides reported here, they present a suitable model for kinetic and mechanistic studies of fibril formation.

Materials and methods

Peptide synthesis

Peptides were assembled on an Applied Biosystems (Foster City, California) 430A automated peptide synthesizer using the base-labile 9-fluorenylmethoxycarbonyl (Fmoc) group for the protection of the α-amino function. Side-chain functionalities were protected by the t-Bu (Asp, Ser, Thr, Tyr), trityl (Asn, Gln), or the Pmc (Arg) group. Synthesis and purification were carried out as described previously (Yang et al., 1994). The identity and purity of the peptides were confirmed by ESI-MS. The masses measured for CspB-1, CspB-2, and CspB-3 were 2,531.1, 3,976.6, and 3,449.5 g/mol, respectively (masses predicted from the sequence: 2,531.9, 3,976.6, 3,448.7).

Sample preparation

All three peptides were found to have optimal solubility if first dissolved in 50% acetonitrile pH 4.0 (adjusted with formic acid, unbuffered), and subsequently diluted to the desired peptide and acetonitrile concentrations.

Table 2. *Overview of results obtained in a series of two screening experiments to assess the formation of amyloid fibrils under different conditions, using congo red binding, EM, and detection of the green birefringence by light microscopy (LM)*[a]

Condition	Method	CspB-1	CspB-2	CspB-3
10% acetonitrile	Congo red	++, ++	++, o	++, ++
	EM	++	++	+
	LM	++, ++	+	++, +
90% acetonitrile	Congo red	++, o	o, ++	++, +
	EM	o	++	o
	LM	++, ++	++, o	o, ++

[a]The final peptide concentration was 1.6 mg/mL for the first congo red experiment carried out under each set of conditions and 2.0 mg/mL for all other experiments. Results: (++) strongly positive, (+) weakly positive, (o) no positive evidence. In addition to the results shown here, fibril formation in 10% acetonitrile was observed in many more experiments carried out with CspB-1 in separate studies (D.K. Wilkins, M. Groß, I. Schofield, & C.M. Dobson, unpubl. results).

Optical spectroscopy

CD spectra were recorded on a Jasco J720 spectropolarimeter using quartz cuvettes of 1 mm pathlength, at 1 nm intervals from 195 to 250 nm. Routinely, CD samples were examined 30 min after dilution from the peptide stock solution containing 50% acetonitrile. Kinetic experiments revealed that, after this time, given the relatively low concentration (0.4 mg/mL) of the CD samples, no time dependent effects could be observed on the timescale of minutes.

Calculation of the β-sheet content was carried out using the ellipticity at 215 nm normalized to a per residue basis (units: deg cm^2/dmol). The highest value observed in this study ($-9,260$ deg cm^2/dmol) was taken to correspond to 100% β structure, which agrees well with the value proposed by other workers ($-9,210$ deg cm^2/dmol at 216 nm (Chen et al., 1974)).

For the congo red binding assay of fibril formation, absorption spectra of a 10 μM solution of the dye in the assay buffer (5 mM phosphate pH 7.4, 0.15 mM NaCl) before and after addition of the peptide solution were recorded on a Perkin Elmer (Foster City, California) Lambda 16 spectrometer in the range of 400 to 700 nm. Typically, 10 μL of the peptide sample were used in a total volume of 1.0 mL.

NMR spectroscopy

All NMR spectra were acquired at ^{1}H frequencies of 500 or 600 MHz on homebuilt NMR spectrometers at the Oxford Centre for Molecular Sciences. One-dimensional (1D) spectra typically contain 8K complex data points. Two-dimensional (2D) experiments were acquired with 2K complex data points in the t_2 dimension, and in phase-sensitive mode using time proportional phase incrementation (TPPI) (Marion & Wüthrich, 1983) for quadrature detection in t_1. Diffusion constants were determined using pulse field gradient experiments (Jones et al., 1997) with 8K complex points. Spectral widths of 8,000 Hz were used for all experiments. For the resonance assignments, DQF-COSY, TOCSY, ROESY, and NOESY spectra were recorded, involving between 512 and 800 t_1 increments with 32 to 128 scans each. The water signal was sup-

pressed either by using presaturation during the 1.2 s relaxation delay or by using a gradient double echo (Schleucher et al., 1994). The mixing times for the TOCSY experiments varied between 23 and 60 ms, and for the NOESY and ROESY experiments between 100 and 260 ms. Data were processed using Felix 2.3 (BIOSYM) on Sun workstations. Typically, the data were zero filled once, and processed with a double exponential window function for the 1D, and a sinebell squared function shifted over 90° for each dimension of the 2D spectra. All spectra were referenced to an internal standard of dioxan at 3.743 ppm.

For the determination of the $^3J_{HN\alpha}$ coupling constants, high resolution DQF-COSY spectra were recorded with 4K complex points zero filled to 8K, and the window functions GM 3.75 and TM 16 4096 4096 applied. The cross peaks were then fitted to simulated antiphase cross sections along the F2 dimension using a procedure implemented in the Felix 2.3 program.

A series of 1D spectra was used to estimate the percentage of peptide visible by solution NMR. These 1D spectra were all acquired with 256 scans on the same 500 MHz NMR spectrometer, in consecutive experiments. The concentration of a tryptophan solution was calculated from its absorbance at 280 nm. The integration of the indole resonances in these 1D spectra from the tryptophan and peptide solutions was used to estimate the concentration of the peptide solutions.

Electron microscopy

Fibril formation and morphology were examined by transmission electron microscopy (EM). Peptide samples were dried onto formvar- and carbon-coated grids and negatively stained with 1% phosphotungstic acid (PTA). Grids were examined in a JEOL JEM-1010 electron microscope at 80 kV excitation voltage.

Light microscopy

Confirmation of the presence of amyloid fibrils in peptide samples was obtained by drying congo red stained fibrils onto glass slides and examining the preparations through a binocular microscope using crossed polarizers. Yellow green birefringence indicates the presence of cross β structure (Cooper, 1974).

X-ray fiber diffraction

Droplets of 10 μL peptide solution were suspended between the ends of two capillaries sealed with wax. While the normal procedure involves evaporation of the solvent over a timescale of $\sim$1 day, the presence of acetonitrile in the samples allowed the droplet to evaporate in approximately 1 h. Diffraction patterns of the remaining solid in the form of two thin needles attached to the ends of the capillaries were collected using a Cu K$_\alpha$ rotating anode equipped with a 180 mm image plate (MAR Research, Hamburg, Germany). The diffraction pattern was analyzed using the MarView software (MAR Research).

Supplementary material in Electronic Appendix

Resonance assignments for all three peptides are provided. Table 1 contains chemical shifts and coupling constants for CspB-1. Table 2 contains chemical shifts for CspB-2. Table 3 contains chemical shifts and coupling constants for CspB-3.

Acknowledgments

References

Arvinte T, Cudd A, Drake AF. 1993. The structure and mechanism of formation of human calcitonin fibrils. *J Biol Chem 268*:6415–6422.

Beyreuther K, Masters CL. 1997. Alzheimer's disease: The ins and outs of amyloid-β. *Nature 389*:677–678.

Blake C, Serpell L. 1996. Synchrotron X-ray studies suggest that the core of the transthyretin amyloid fibril is a continuous β-sheet helix. *Structure 4*:989–998.

Booth DR, Sunde M, Bellotti V, Robinson CV, Hutchinson WL, Fraser PE, Hawkins PN, Dobson CM, Radford SE, Blake CCF, Pepys MB. 1997. Instability, unfolding, and aggregation of human lysozyme variants underlying amyloid fibrillogenesis. *Nature 385*:787–793.

Bycroft M, Hubbard TJP, Proctor M, Freund SMV, Murzin AG. 1997. The solution structure of the S1 RNA binding domain: A member of an ancient nucleic acid-binding fold. *Cell 88*:235–242.

Chen Y-H, Yang JT, Chau KH. 1974. Determination of the helix and beta form of proteins in aqueous solution by circular dichroism. *Biochemistry 13*:3350–3359.

Chiti F, Webster P, Taddei N, Stefani M, Ramponi G, Dobson CM. 1999. Designing conditions for in vitro formation of amyloid fibrils. *Proc Natl Acad Sci USA 96*:3590–3594.

Cooper JH. 1974. Selective amyloid staining as a function of amyloid composition and structure. *Lab Invest 31*:232–238.

Deleage G, Roux B. 1987. An algorithm for protein secondary structure prediction based on class prediction. *Protein Eng 1*:289–294.

Fink AL. 1998. Protein aggregation: Folding aggregates, inclusion bodies and amyloid. *Folding Design 3*:R9–R23.

Geourjon C, Deleage G. 1995. Significant improvements in protein secondary structure prediction by prediction from multiple alignments. *Comput Appl Biosci 11*:681–684.

Gibrat JF, Garnier J, Robson B. 1987. Further developments of protein secondary structure prediction using information-theory—New parameters and consideration of residue pairs. *J Mol Biol 198*:425–443.

Graumann P, Marahiel MA. 1997. Effects of heterologous expression of CspB, the major cold shock protein of *Bacillus subtilis*, on protein synthesis in *Escherichia coli. Mol Gen Genet 253*:745–752.

Graumann PL, Marahiel MA. 1998. A superfamily of proteins that contain the cold-shock domain. *Trends Biochem Sci 23*:286–290.

Groß M. 1996. Linguistic analysis of protein folding. *FEBS Lett 390*:249–252.

Groß M, Dobson CM. 1997. Folding of nascent protein chains. *Chimia 51*:443.

Guijarro JI, Sunde M, Jones JA, Campbell ID, Dobson CM. 1998. Amyloid fibril formation by an SH3 domain. *Proc Natl Acad Sci USA 95*:4224–4228.

Han H, Weinreb PH, Lansbury PT. 1995. The core Alzheimer's peptide NAC forms amyloid fibrils which seed and are seeded by β-amyloid: Is NAC a common trigger of target in neurodegenerative disease? *Chem Biol 2*:163–169.

Harrison PM, Bamborough P, Daggett V, Prusiner SB, Cohen FE. 1997. The prion folding problem. *Curr Op Struct Biol 7*:53–59.

Jiménez JL, Guijarro JI, Orlova E, Zurdo J, Dobson CM, Sunde M, Saibil HR. 1999. Cryo-electron microscopy structure of an SH3 amyloid fibril and model of the molecular packing. *EMBO J 18*:815–821.

Jones JA, Wilkins DK, Smith LJ, Dobson CM. 1997. Characterization of protein unfolding by NMR diffusion measurements. *J Biomol NMR 10*:199–203.

Kelly JW. 1997. Amyloid fibril formation and protein misassembly: A structural quest for insights into amyloid and prion diseases. *Structure 5*:595–600.

Kurochkin IV. 1998. Amyloidogenic determinant as a substrate recognition motif of insulin-degrading enzyme. *FEBS Lett 427*:153–156.

Lazo ND, Downing DT. 1998. Amyloid fibrils may be assembled from β-helical protofibrils. *Biochemistry 37*:1731–1735.

Levin JM, Robson B, Garnier J. 1986. An algorithm for secondary structure determination in proteins based on sequence similarity. *FEBS Lett 205*:303–308.

Litvinovich SV, Brew SA, Aota S, Akiyama SK, Haudenschild C, Ingham KC. 1998. Formation of amyloid-like fibrils by self-association of a partially unfolded fibronectin type III module. *J Mol Biol 280*:245–258.

Marion D, Wüthrich K. 1983. Application of phase-sensitive two-dimensional correlated spectroscopy (COSY) for measurements of H1-H1 spin-spin coupling constants in proteins. *Biochem Biophys Res Comm 113*:967–974.

Pepys MB, Hawkins PN, Booth DR, Vigushin DN, Tennent GA, Soutar AK, Totty N, Nguyen O, Blake CCF, Terry CJ, Feest TG, Zalin AM, Hsuan JJ. 1993. Human lysozyme gene mutations cause hereditary systemic amyloidosis. *Nature 362*:553–556.

Peterson S, Klabunde T, Lashuel H, Purkey H, Sacchettini J, Kelly J. 1998. Inhibiting transthyretin conformational changes that lead to amyloid fibril formation. *Proc Natl Acad Sci USA 95*:12956–12960.

Pillot T, Lins L, Goethals M, Vanloo B, Baert J, Vandekerckhove J, Rosseneu M, Brasseur R. 1997. The 118–135 peptide of the human prion protein forms amyloid fibrils and induces liposome fusion. *J Mol Biol 274*:381–393.

Plaxco KW, Morton CJ, Grimshaw SB, Jones JA, Pitkeathly MC, Campbell ID, Dobson CM. 1997. The effects of guanidine hydrochloride on the random coil conformations and NMR chemical shifts of the peptide series GGXGG. *J Biomol NMR 10*:221–230.

Plaxco KW, Simons KT, Baker D. 1998. Contact order, transition state placement and the refolding rates of single domain proteins. *J Mol Biol 277*:985–994.

Schindelin H, Marahiel MA, Heinemann U. 1993. Universal nucleic acid binding domain revealed by crystal structure of the *Bacillus subtilis* major cold-shock protein. *Nature 364*:164–168.

Schindler T, Herrler M, Marahiel MA, Schmid FX. 1995. Extremely rapid protein folding in the absence of intermediates. *Nature Struct Biol 2*:663–673.

Schindler T, Schmid FX. 1996. Thermodynamic properties of an extremely rapid protein folding reaction. *Biochemistry 35*:16833–16842.

Schleucher J, Schwendinger M, Sattler M, Schmidt P, Schedletzky O, Glaser SJ, Sorensen OW, Griesinger C. 1994. A general enhancement scheme in heteronuclear multidimensional NMR employing pulsed-field gradients. *J Biomol NMR 4*:301–306.

Schnuchel A, Wiltscheck R, Czisch M, Herrler M, Willimsky G, Graumann P, Marahiel MA, Holak TA. 1993. Structure in solution of the major cold-shock protein from *Bacillus subtilis. Nature 364*:169–171.

Serpell LC. 1995. Structural studies of amyloid proteins. University of Oxford.

Serrano L. 1995. Comparison between the phi distribution of the amino acids in the protein database and NMR data indicates that amino acids have various phi propensities in the random coil conformation. *J Mol Biol 254*:322–333.

Smith LJ, Fiebig KM, Schwalbe H, Dobson CM. 1996. The concept of a random coil: Residual structure in peptides and denatured proteins. *Folding Design 1*:R95–R106.

Sunde M, Blake C. 1997. The structure of amyloid fibrils by electron microscopy and X-ray diffraction. *Adv Prot Chem 50*:123–159.

Westermark P, Wernstedt C, Wilander E, Hayden DW, O'Brien TD, Johnson KH. 1987. Amyloid fibrils in human insulinoma and islets of Langerhans of the diabetic cat are derived from a neuropeptide-like protein also present in normal islet cells. *Proc Natl Acad Sci USA 84*:3881–3885.

Wishart DS, Bigam CG, Holm A, Hodges RS, Sykes BD. 1995. ^{1}H, ^{13}C and ^{15}N random coil NMR chemical shifts of the common amino acids. I. Investigations of nearest-neighbor effects. *J Biomol NMR 5*:67–81.

Yang JJ, Pitkeathly M, Radford SE. 1994. Far-UV circular dichroism reveals a conformational switch in a peptide fragment from the β sheet of hen lysozyme. *Biochemistry 33*:7345–7353.

Amyloid fibrils from muscle myoglobin

Even an ordinary globular protein can assume a rogue guise if conditions are right.

The sequence of amino acids in a natural protein determines the way in which it folds up into its unique biologically active 'native' conformation[1]. But we show here that myoglobin, the archetypal globular protein[2], can convert into an alternative and radically different structure that closely resembles the amyloid and prion aggregates seen in pathological conditions such as Alzheimer's and Creutzfeldt–Jakob diseases[3–6]. This most striking example of such a structural transition provides compelling evidence for the idea that amyloid represents a generic form of polypeptide conformation, but one that evolution has ensured is not normally formed in living systems[7,8].

Myoglobin (Fig. 1a) is a compact and highly soluble protein without any native-state properties to suggest that it has a predisposition to form amyloid fibrils. Whereas the latter are characteristically rich in β-sheets, native myoglobin lacks any elements of such structure and has most of its sequence arranged in well-defined α-helices. Moreover, all partially folded states of the protein characterized so far are significantly helical[9], although, as with most proteins, there is evidence for the presence of more extended conformations in aggregates and precipitates[9,10].

In a screening process, in which pH, temperature and buffers were varied, we found that incubation of apomyoglobin (the protein without its haem group) in 50 mM sodium borate, pH 9.0 at 65 °C, conditions under which the native fold is substantially destabilized, resulted in the formation of large quantities of fibrillar structures (Fig. 1b). Solutions of these fibrils gave rise to a far-ultraviolet circular-dichroism spectrum containing a single minimum at 215 nm (Fig. 1c), which is diagnostic for the presence of β-structure. Moreover, an anisotropic X-ray diffraction pattern was obtained with characteristic 'cross-β' reflections at 4.63 ± 0.08 and 10.11 ± 1.23 Å (Fig. 1d).

These results indicate that myoglobin fibrils contain β-strands that are oriented perpendicular to the main fibre axis[5] and, together with the properties of the fibril-containing solutions in tinctorial assays using thioflavin T and Congo Red, indicate that these fibrils are indistinguishable in their core structure from disease-related amyloid fibrils[5].

Our findings for myoglobin provide strong evidence that the sequences of polypeptides associated with amyloid or prion diseases need not be fundamentally distinct from those of other proteins by
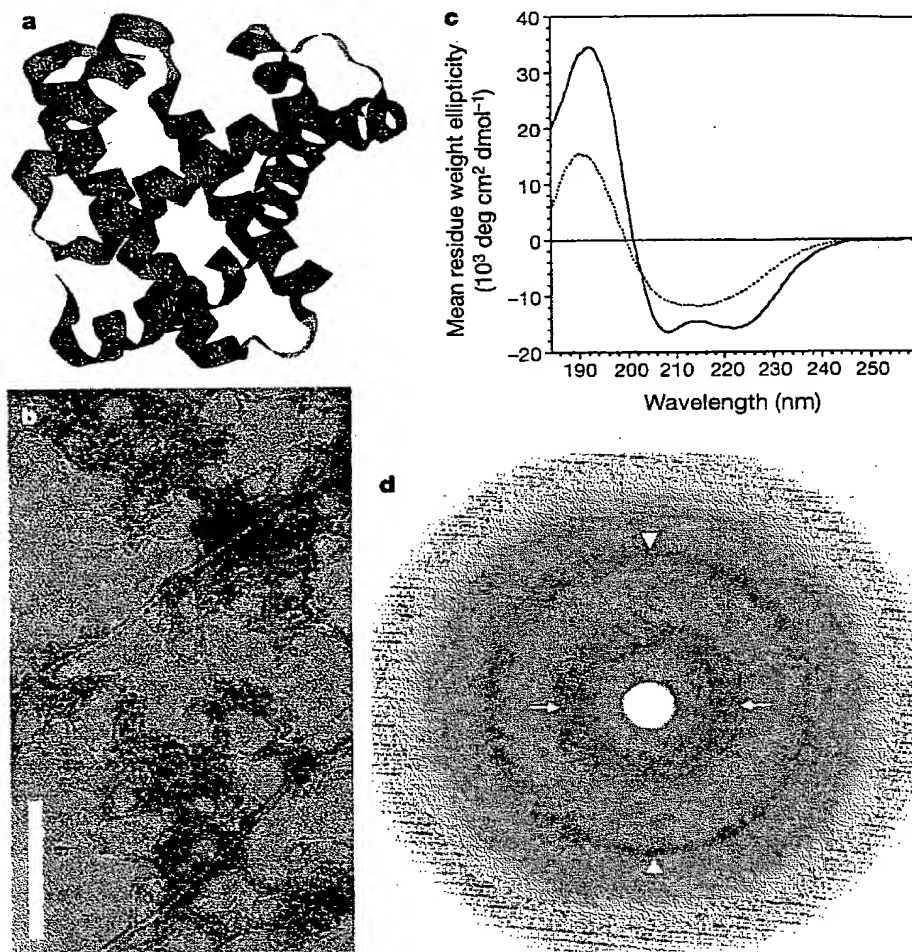
Figure 1 Structure of native and fibrillar myoglobin. **a**, Backbone representation of native myoglobin[11]; α-helical residues are picked out in red. **b**, Electron micrograph of fibrils formed from horse skeletal-muscle myoglobin after haem extraction[12] and stained with uranyl acetate. Scale bar, 300 nm. **c**, Far-ultraviolet circular-dichroism spectra at 22 °C of freshly dissolved apomyoglobin (continuous line) and purified fibrils after incubation for 25 days (dotted line). **d**, X-ray diffraction pattern of fibres obtained using an 18-cm imaging plate detector (MarResearch) with a Rigaku RU200 rotating anode. Arrowheads (on the meridian) indicate the 4.63-Å reflection; arrows indicate the 10.11-Å reflection.

having any explicit coding for the cross-β structure[7]. But how can a polypeptide chain fold into two different, well-ordered states? In the native state of a globular protein such as myoglobin (Fig. 1a), side-chain interactions are crucial in defining the unique and characteristic main-chain fold[1]. We suggest that, in contrast, the cross-β conformation is dominated by main-chain interactions that are common to different polypeptides; hence sequence effects are much less significant in determining the amyloid core structure. The latter is instead likely to be favoured by the inherent physical-chemical properties of the otherwise disordered polypeptide chains as they aggregate slowly under specific solution conditions in which

the native state is unstable.

We believe that the ability of natural protein sequences (which represent only a small fraction of all possible sequences) to fold efficiently into cooperative globular structures, together with other strategies such as employing molecular chaperones, is a very effective evolutionary adaptation to suppress amyloid formation in vivo. Conditions compromising such protective mechanisms, including ageing or mutational changes, may sometimes allow even a highly selected natural sequence to revert to its alternative conformation.

This proposal enables the basic principle of protein folding, namely that there is an unambiguous relationship between the

amino-acid sequence and the structure in the native state[1], to be reconciled with the evidence that even a protein such as myoglobin can adopt the fundamentally different but highly organized structure present in amyloid fibrils.

Marcus Fändrich, Matthew A. Fletcher, Christopher M. Dobson

*Oxford Centre for Molecular Sciences,
New Chemistry Laboratory, University of Oxford,
South Parks Road, Oxford OX1 3QT, UK
e-mail: chris.dobson@chem.ox.ac.uk*

1. Anfinsen, C. B. *Science* 181, 223–230 (1973).
2. Kendrew, J. C. *et al. Nature* 185, 422–427 (1960).
3. Tan. S. Y. & Pepys, M. B. *Histopathology* 25, 403–414 (1994).
4. Rochet, J. C. & Lansbury, P .T. Jr *Curr. Opin. Struct. Biol.* 10, 60–68 (2000).
5. Sunde, M. & Blake, C. C. F. Q. *Rev. Biophys.* 31, 1–39 (1998).
6. Prusiner, S. B. *Proc. Natl Acad. Sci. USA* 95, 13363–13383 (1998).
7. Dobson, C. M. *Trends Biochem. Sci.* 24, 329–332 (1999).
8. Chiti, F. *et al. Proc. Natl Acad. Sci. USA* 96, 3590–3594 (1999).
9. Eliezer, D., Yao, J., Dyson, H. J. & Wright, P. E. *Nature Struct. Biol.* 5, 148–155 (1998).
10. Smeller, L., Rubens, P. & Heremans, K. *Biochemistry* 38, 3816–3820 (1999).
11. Evans, S. V. & Brayer, G. D. *J. Biol. Chem.* 263, 4263–4268 (1988).
12. Teale, F. W. *J. Biochim. Biophys. Acta* 35, 543 (1959).

Pattern formation

Spiral cracks without twisting

A fascinating class of patterns, often encountered in nature as meandering cracks on rocks, dried-out fields and tectonic plates, is produced by the fracture of solids[1]. Here we describe the observation and modelling of an unusual type of pattern consisting of spiral cracks in fragments of a thin layer of drying precipitate. We find that this symmetry-breaking cracking mode arises naturally not from twisting forces, but from a propagating stress front induced by the fold-up of the fragments.

Fractured surfaces and lines[2–6] typically show a cellular and hierarchical pattern. Twisting forces produce a spiral fracture, like that often seen in a tibia bone broken in a skiing accident[7]. However, spiral cracks can also be created in other situations, as we show here by drying a fine aqueous suspension of precipitate. During drying, the suspension solidifies and later fragments into isolated parts (Fig. 1a).

Surprisingly, for very fine precipitates in a solidified layer of thickness between 0.2 and 0.5 mm, regular spiral as well as circular cracking pathways show up inside the fragments (Fig. 1b). Depending on the grain size, precipitate type and layer thickness, the size of the spirals varies widely from several hundred micrometres to a few millimetres. To the naked eye, they look like small dots, but their detail is revealed under a microscope (Fig. 1c). These spiral cracks do not occur in one particular material — we were able to generate them in three different precipitates, from nickel phosphate $Ni_3(PO_4)_2$, ferric ferrocyanide $Fe_4[Fe(CN)_6)]_3$ and ferric hydroxide $Fe(OH)_3$.
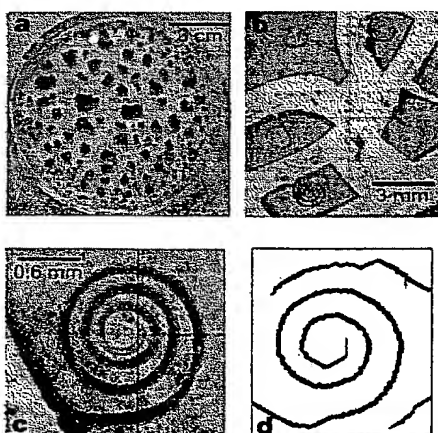
Careful *in situ* observation suggested a mechanism for the formation of these cracks. The spirals and circle-shaped structures form only after the fragmentation process is over. Owing to the humidity gradient across the thickness, the fragments gradually fold up and detach from the substrate, generating large tensile stresses in the radial direction, at and normal to the front of detachment. The extent of the attached area shrinks as the ring-shaped front advances inwards as a result of ongoing desiccation.

When the stress at the front exceeds the material strength, a crack is nucleated. As the nucleation is seldom symmetrical with respect to the boundaries, the crack tends to propagate along the front in only one direction, where more stresses can be released. By the time the crack growth completes a cycle, the front has already advanced, leading eventually to an inward spiral crack. As the stresses are concentrated at the layer–substrate interface, the spiral is confined there, with a typical penetration of 20–60% of the thickness.

The fact that the patterns are largely spiral suggests that crack propagation is favoured over nucleation, otherwise we would see more cylindrical concentric cracks. Although in a few instances we did observe this type of pattern, the majority are spiral in structure.

To test the proposed mechanism, we implemented it in a mesoscopic computer model[8] that describes fracture on a frictional substrate. In this model, the grains in the layer are represented by blocks on a triangular lattice, interconnected among neighbours by springs. The system is pre-strained, and then relieved quasi-statically in a physical way. The relaxation is dictated by the competition between stick-and-slip and bond-breaking.

Focusing on the post-fragmentation process, we imposed a circular, inwardly propagating stress field to mimic the advancing detachment front. In a rather narrow parameter region, the spiral cracks were successfully reproduced (Fig. 1d). More tightly bound spirals can be obtained for smaller penetration depth, in agreement with experiment and prediction based on screening effects in the stress field. Other evidence has also been reported for the formation of similar spiral crack patterns under specific conditions[9].

K.-t. Leung*, L. Józsa†, M. Ravasz‡, Z. Néda‡§

*Institute of Physics, Academia Sinica, Taipei, Taiwan 11529, Republic of China
Departments of †Chemistry and ‡Physics, Babes-Bolyai University, Cluj, RO-3400, Romania
§Department of Physics, University of Notre Dame, Notre Dame, Indiana 46556, USA
e-mail: zneda@nd.edu*

1. Lawn, B. *Fracture of Brittle Solids* 2nd edn (Cambridge Univ. Press, New York, 1993).
2. Skjeltorp, A. T. & Meakin, P. *Nature* 335, 424–426 (1988).
3. Yuse, A. & Sano, M. *Nature* 362, 329–331 (1993).
4. Groisman, A. & Kaplan, E. *Europhys. Lett.* 25, 415–420 (1994).
5. Bai, T., Pollard, D. D. & Gao, H. *Nature* 403, 753–756 (2000).
6. Shorlin, K. A., de Bruyn, J. R., Graham, M. & Morris, S.W. *Phys. Rev. E* 61, 6950–6957 (2000).
7. Bostman, O. M. *J. Bone Joint Surg.* 68, 462–466 (1986).
8. Leung, K.-t. & Neda, Z. *Phys. Rev. Lett.* 85, 662–665 (2000).
9. Xia, Z. C. & Hutchinson, J. W. *J. Mech. Phys. Solids* 48, 1107–1131 (2000).

Figure 1 Spiral cracks revealed at small scales. **a**, Typical fragmentation pattern of nickel phosphate precipitate after desiccation in a Petri dish. **b**, Spiral and circular structures obtained inside the fragments. **c**, Close-up of a spiral crack. **d**, Computer-simulated spiral crack obtained using a mesoscopic spring-block model.

Polynesian origins

Slow boat to Melanesia?

The origin of the Polynesian islanders and of the Austronesian languages that they speak has been debated for more than 200 years. Diamond has presented the predominantly held modern viewpoint, described as the 'express train to Polynesia' model, which proposes that the ancestors of the Polynesians were early farmers who dispersed south from a homeland in South China/Taiwan, through Island Southeast Asia (replacing an indigenous 'Australoid' hunter-gatherer population), and then on east, out into the Pacific — all within the past 6,000 years[1]. However, evidence is accumulating from several genetic markers that Polynesian lineages have a much deeper ancestry within tropical Island Southeast Asia than this hypothesis would suggest. The new evidence implies that the Polynesians originated not in China/Taiwan, but in eastern Indonesia, somewhere between Wallace's line and the island of New Guinea.

Freezing of a Fish Antifreeze Protein Results in Amyloid Fibril Formation

Steffen P. Graether, Carolyn M. Slupsky, and Brian D. Sykes
Canadian Institute of Health Research Group in Protein Structure and Function, Department of Biochemistry and Protein Engineering Network of Centres of Excellence, University of Alberta, Edmonton, Alberta, T6G 2H7 Canada

ABSTRACT   Amyloid is associated with a number of diseases including Alzheimer's, Huntington's, Parkinson's, and the spongiform encephalopathies. Amyloid fibrils have been formed in vitro from both disease and nondisease related proteins, but the latter requires extremes of pH, heat, or the presence of a chaotropic agent. We show, using fluorescence spectroscopy, electron microscopy, and solid-state NMR spectroscopy, that the α-helical type I antifreeze protein from the winter flounder forms amyloid fibrils at pH 4 and 7 upon freezing and thawing. Our results demonstrate that the freezing of some proteins may accelerate the formation of amyloid fibrils.

INTRODUCTION

Amyloidosis describes the presence of proteinaceous deposits with specific morphological, staining, and structural characteristics. The existence of these insoluble and proteolytically resistant deposits can seriously interfere with normal organ function (Pepys, 2001). Amyloid deposits have been associated with a number of diseases, including Alzheimer's, Huntington's, Parkinson's, AA amyloidosis, type II diabetes, dialysis-related amyloidosis, and scrapie. When stained with traditional dyes, amyloid deposits appear amorphous. However, when stained with Congo Red and viewed through cross-polarizing lenses, amyloid deposits show a characteristic green birefringence, which suggests an underlying structure. Under an electron microscope, the fibrils appear unbranched and have a diameter of 50–130 Å (Serpell et al., 1997). X-ray diffraction studies reveal that these fibrils have a "cross-β" structure, wherein the protein aggregates as β-strands forming a sheet that winds around the fibril axis in a helical manner (Serpell et al., 1997). Solid-state NMR work has refined the fibril model by showing that the β-amyloid peptides form parallel β-sheets (Balbach et al., 2002; Benzinger et al., 2000), although an antiparallel arrangement has also been detected for a shorter β-amyloid peptide (Balbach et al., 2000). Other NMR experiments have demonstrated that the backbone conformation differs from the classical β-sheet (Costa et al., 1997; Spencer et al., 1991). Despite these similar morphological features, no consistent similarity in sequence, structure, or function has been found for proteins that are able to form amyloid fibrils (Kisilevsky, 2000; Chiti et al., 2001; Dobson, 1999).

One of the first clues that the formation of amyloid fibrils may not be limited to the disease state was the study on the SH3 domain of the phosphatidylinositol kinase (Guijarro et al., 1998). Exposure of this protein to low pH resulted in the formation of a gel with morphological properties similar to amyloid fibrils. This has also been repeated with a number of other, nonpathological proteins including fibronectin (Litvinovich et al., 1998), cold-shock protein B (Gross et al., 1999), and myoglobin (Fandrich et al., 2001).

Type I antifreeze protein (AFP, also known as thermal hysteresis protein and as ice-structuring protein) is found at relatively high concentrations in the circulatory system (10–15 mg/mL) and in the skin of fish living in subzero seawater, and protects the organism from macromolecular ice growth by adsorption inhibition (Fletcher et al., 2001). Structural studies have revealed that the 37-residue protein forms an α-helical structure (Sicheri and Yang, 1995; see Fig. 1). The role of hydrogen bonds and van-der-Waals forces in ice binding has been extensively studied (Jia and Davies, 2002); however, their relative contribution to the interaction remains unclear.

During our studies of the AFP mechanism, we found that the winter flounder type I AFP in solution formed a translucent gel upon freezing and thawing at physiological pH and below. It has been established that gel formation of a protein at or above the critical concentration of polymerization (Harper and Lansbury, 1997) may indicate the formation of amyloid fibrils. To determine if the gel was amyloidotic in nature, we examined three properties specific to amyloid: morphology by electron microscopy, fluorescence staining by the amyloid-specific dye Thioflavin T (ThT), and structural characteristics by solid-state ^{13}C-NMR spectroscopy. The data presented here demonstrate that type I AFP can be converted into amyloid fibrils upon freezing and thawing, conditions appropriate to its physiological function.

MATERIALS AND METHODS

Preparation of AFP fibril

The wild-type winter flounder AFP HPLC-6 was synthesized according to standard solid-phase peptide synthesis methods as described previously (Hodges et al., 1988). For ^{13}C-labeled samples, a ^{13}Cα-alanine residue (2-^{13}C-alanine, Cambridge Isotopes Laboratories, Andover, MA) was incorporated at position 17 (Fig. 1).
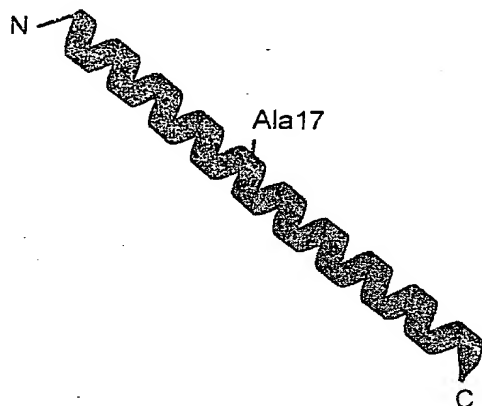
FIGURE 1 Structure of type 1 AFP. A ribbon diagram of the type I AFP crystal structure (PDB code 1wfb, chain B; see Sicheri and Yang, 1995). The protein is 37 residues long, with 23 residues consisting of alanine. The location of the single $^{13}C\alpha$-alanine is labeled.

For the preparation of unlabeled antifreeze protein for use with the fluorescence experiments, 3 mg of protein was dissolved in 31 μL of H_2O. The pH was adjusted to ~4 by the addition of 9 μL of 100 mM NaOH, resulting in a final protein concentration of 75 mg/mL (23 mM). An aliquot of the sample was stored at 4°C as a negative control. The remaining aliquots were frozen and thawed between one and three times.

For the preparation of labeled protein for NMR experiments, 9 mg of $^{13}C\alpha$-Ala17 type I AFP was dissolved in 90 μL of H_2O. To adjust the pH to ~4, 30 μL of 100 mM NaOH was added, giving a final concentration of 75 mg/mL (23 mM). The sample was frozen and thawed as indicated in Fig. 4.

Electron microscopy

Electron micrographs were acquired on a Hitachi Transmission Electron Microscope H-7000 (Tokyo) operating at a 75-kV excitation voltage. The sample was prepared by applying 3 μL of ~50 mg/mL protein gel on a Formvar grid and subsequently dried. The gel was negatively stained with 2% uranyl acetate.

ThT fluorescence

ThT fluorescence was performed as described by LeVine (1999). Briefly, 1 μg of protein was mixed with 1 mL of 5 μM ThT in 50 mM glycine-NaOH, pH 8.5. The fluorescence of the sample was measured on a Shimadzu RF5301-PC fluorescence spectrophotometer (Kyoto, Japan) with the emission intensity traced from 460 to 520 nm with a 10-nm slit width using an excitation wavelength of 450 nm with a 5-nm slit width. Relative fluorescence values are reported at 482 nm. The three negative controls consisted of ThT alone, AFP fibril alone, or AFP in solution with 5 μM ThT.

NMR spectroscopy

The NMR spectra were collected at 7.04 Tesla corresponding to a ^{13}C Larmor frequency of 75.416 MHz on a Varian Unity Spectrometer (Palo Alto, CA) equipped with a Varian/Chemagnetics double-resonance MAS probe with a 5.0-mm PENCIL-I MAS rotor. For the ^{13}C-CP/MAS experiments, the cross-polarization contact time was 3.0 ms during which the ^{1}H decoupling field strength was 78.1 kHz. During acquisition, the decoupling field strength was reduced to 55.3 kHz. 13,312 transients were collected with a recycle delay of 5 s. The proton 90° pulsewidth was

calibrated to be 3.6 μs. For the ^{13}C-MAS experiments, a ^{1}H decoupler field strength of 15.6 kHz was applied to 144 or 512 transients with a recycle delay of 3 s. All MAS experiments were collected with 2972 complex data points, a sweepwidth of 37,140 Hz, and performed with the sample spinning at 3.333 kHz. Chemical shifts were referenced relative to the carbon chemical shift of 2,2'-dimethyl-2-silapentane-5-sulfonate (0 ppm; see Wishart et al., 1995).

RESULTS

Electron microscopy reveals unbranched fibrils

Electron microscopy was used to examine uranyl acetate stained gel preparations of type I AFP. Fig. 2 shows unbranched fibrils that are ~50 Å in diameter, which is in agreement with previous studies on fibrils in amyloid deposits (Serpell et al., 1997). In addition, studies have shown that these fibrils associate into larger, mature fibrils, where several protofilaments coil around one another (Chiti et al., 1999). This is illustrated for type I AFP in Fig. 2 B.

Type I AFP gel binds the fluorescent dye ThT

To provide further evidence that the type I AFP fibrils were amyloidotic in nature, we examined the AFP gel in the
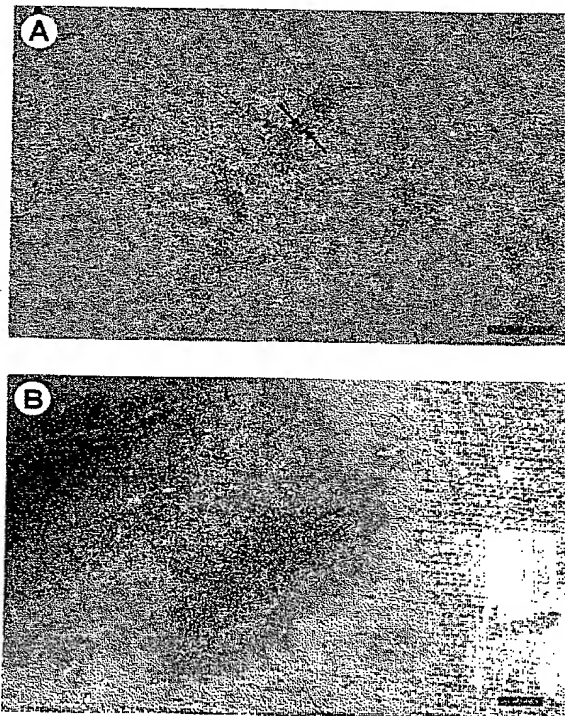

FIGURE 2 Transmission electron micrographs of AFP gel. Uranyl acetate stained preparations of the AFP gel were examined under an electron microscope to determine its nature. (A) Fibrils formed after freezing and thawing a 75 mg/mL, pH 4 sample three times. The arrows show an individual fibril with a diameter of ~50 Å. (B) Protofilaments. Scale bars, 100 nm.

presence of the fluorescent dye ThT. ThT undergoes a specific excitation and emission redshift when bound to amyloid fibrils (LeVine, 1999). Congo Red (Puchtler et al., 1962), a stain commonly used for detecting amyloid fibrils, was not employed inasmuch as it has been shown to bind soluble proteins including β-helical proteins (Khurana et al., 2001). Fig. 3 shows a bar graph demonstrating the increase in fluorescence intensity over time with successive freeze-and-thaw cycles. Immediately after one freeze/thaw cycle, there is little change in the fluorescence intensity. Subsequent freeze/thaw cycles increased the fluorescence signal, suggesting that more of the protein was being converted into amyloid fibril. Similar results were obtained with type I AFP at pH 7, 100 mM NaCl (data not shown). In addition, the warming and cooling of a type I AFP solution between 5°C and 25°C did not cause a gel to form. These two results demonstrate that it is the freeze/thaw procedure and not the low pH or temperature cycling that promote amyloid formation. The control sample of type I AFP that was not frozen had approximately the same fluorescence as the ThT dye alone. Interestingly this sample, upon storage at 4°C for several days before the fluorescence experiments, had also become gel-like, but was transparent and not firm like the translucent, amyloidotic gel.

Solid-state ^{13}C-NMR spectroscopy shows a β-sheet structure

The third assessment for amyloid formation is the presence of β-sheet structure. To follow changes in protein conformation during freezing and thawing, ^{13}C-NMR was used as ^{13}Cα chemical shifts are especially sensitive to secondary structure; a positive deviation from random coil chemical
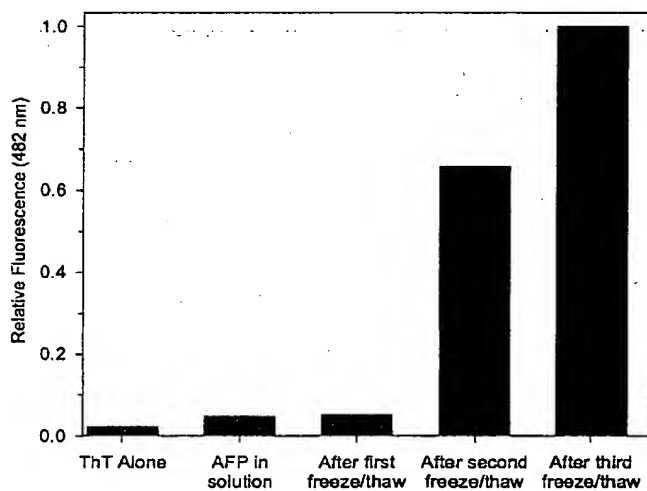

FIGURE 3   ThT fluorescence of fibrillar AFP and controls. Samples of the AFP gel after various stages of freezing and thawing were treated with the amyloid-specific dye ThT. A bar graph shows the normalized fluorescence emission maximum at 482 nm after excitation at 450 nm.

shifts (51.7 ppm for alanine) is indicative of an α-helical conformation whereas a negative deviation is indicative of β-sheet conformation (Wishart et al., 1994). Because 23 of the 37 residues in type I AFP are alanine, the protein was synthesized with a single ^{13}Cα label at position Ala17 to simplify analysis (Fig. 1). Solid-state ^{13}C-1D magic-angle spinning direct polarization (^{13}C-MAS) experiments revealed that before freezing, the protein was α-helical (54.1 ppm chemical shift at 20°C) (Fig. 4 A). This value is similar to the previously measured chemical shift of 54.5 ppm at 21°C (Graether et al., 2001). Upon freezing, the signal was lost (Fig. 4 A). A cross-polarization/magic-angle spinning (^{13}C-CP/MAS) spectrum subsequently taken at −20°C (Fig. 4 B) indicated that the peptide remained α-helical in ice with a chemical shift of 55.1 ppm. This also agrees with experiments demonstrating that the protein remains α-helical when supercooled (Graether et al., 2001) and rules out denaturation during the freezing process as the cause of fibril formation.

Upon thawing the sample at 20°C, the ^{13}C-MAS spectrum revealed a lower intensity than before freezing. This intensity decreased over 20 h (at 20°C) during which a ^{13}C-CP/MAS spectrum was taken. Three peaks were found centered at 54.0, 51.5, and 50.9 ppm. The peak at 54.0 ppm is consistent with an α-helical structure, whereas the peaks at 51.5 and 50.9 are consistent with a β-sheet structure. The heterogeneity in β-sheet chemical shifts may indicate that the fibril is dynamic. Refreezing of the sample produced a spectrum with chemical shifts of 55.0 and 51.4 ppm. The peak at 51.4 ppm is consistent with the chemical shift observed for an alanine residue in a parallel β-sheet structure found in amyloidotic prion protein fragments (Laws et al., 2001). Further thawing and freezing of the protein results in a total loss of intensity in the ^{13}C-MAS experiment indicating a loss of free protein. Concomitantly, the ^{13}C-CP/MAS experiments revealed an increase in the amount of protein in the parallel β-sheet conformation. Interestingly, at a certain point the peak at 55 ppm appears to change little upon freezing and thawing. This was also observed for the prion protein and may be due to the trapping of the α-helical form of AFP in the gel matrix.

DISCUSSION

Conformational stability and amyloidogenesis

It has been shown that destabilization of the native conformation of several proteins render it prone to amyloid formation (Kelly, 1998; Dobson, 2001; Chiti et al., 1999). To induce amyloid formation, these proteins require unusual conditions such as extremes of pH, high concentrations of chaotropic agents, such as TFE, or high temperatures (Guijarro et al., 1998; Chiti et al., 2000; Fandrich et al., 2001; Chiti et al., 2001; Bucciantini et al., 2002; Litvinovich
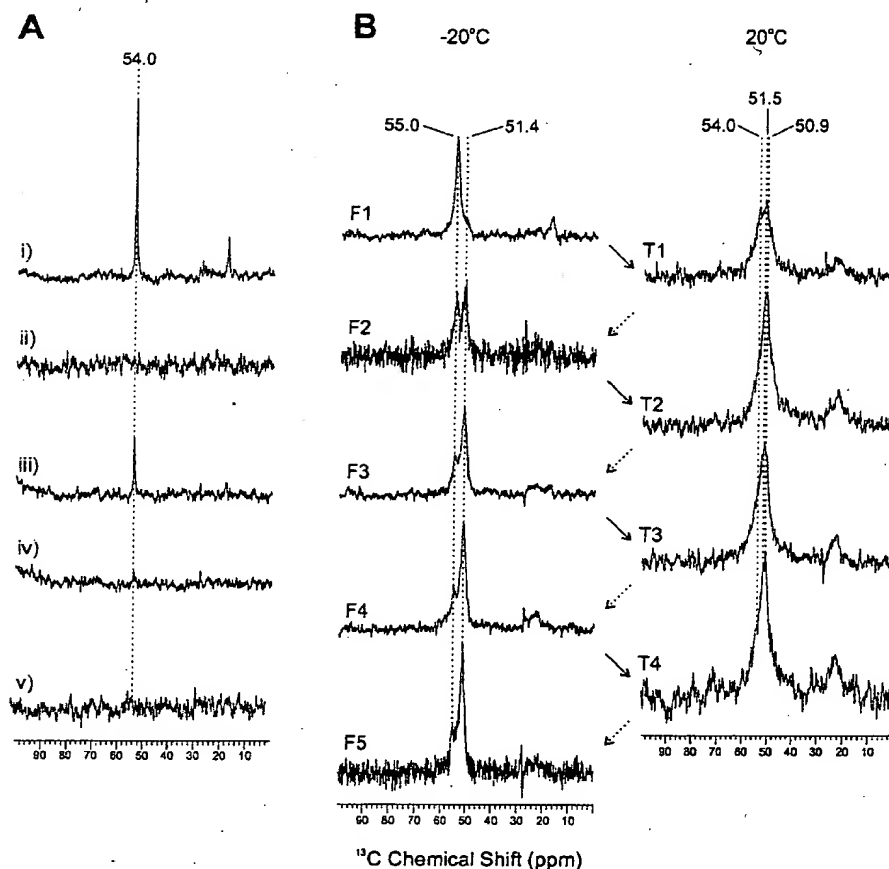
FIGURE 4 ^{13}C-NMR spectra of type I AFP. The conformation of the type I AFP was examined after sequential freeze/thaw cycles by following the ^{13}Cα-Ala17 chemical shift. Values greater than 51.7 ppm indicate that the residue is in an α-helical conformation, whereas lesser values indicate β-strand conformation. Numbers indicate the chemical shift of the ^{13}Cα-Ala17 peak(s). (A) ^{13}C-MAS direct polarization: (i) Before first freeze, 20°C; (ii) Frozen, −20°C; (iii) 30 min after first thaw, 20°C; (iv) 20 h after first thaw, 20°C; and (v) After second thaw, 20°C. (B) ^{13}C-CP/MAS spectra of AFP at −20°C (left) and 20°C (right). The arrows indicate the spectra after sequential freeze (dashed line) and thaw (solid line) cycles. The number indicates the cycle of freezing (F1–5) or thawing (T1–5). Chemical shifts are referenced to 2,2′-dimethyl-2-silapentane-5-sulfonate at 0 ppm (Wishart et al., 1995).

et al., 1998). For type I AFP, amyloid formation can occur at neutral pH and physiological salt concentrations suggesting that the chemical environment is not responsible for amyloid formation for this protein.

Antifreeze proteins have a number of unusual properties. Analysis of the type I AFP amino-acid sequence using the program SEQSEE (Wishart et al., 1994) predicts that due to its high hydrophobicity (68% of the residues are hydrophobic), the protein forms multimers and is therefore not expected to be soluble. Nonetheless, type I AFP can dissolve to a high concentration (>50 mg/mL) and remain monomeric and α-helical, presumably because of its high alanine content (23 of 37 residues). Interestingly, a de novo designed helical peptide was shown to form fibrils at neutral pH (Fezoui et al., 2000). However, this peptide appeared to be only partially folded at pH 7.4 whereas at pH 3.6, where the peptide was most stable, fibril formation was not favored. This is in direct contrast to type I AFP, which was able to form fibrils at neural and acidic pHs, and appears to have an increase in stability as the temperature is decreased (Graether et al., 2001).

For the most part, amyloid fibril formation is associated with disease states. However, there are examples where amyloid formation can be beneficial to an organism. In *Escherichia coli* and *Salmonella* spp., a class of proteins known as curli are responsible for forming extracellular amyloid-like fibers which are responsible for colonization of inert surfaces, biofilm formation, and mediation of binding to host proteins (Chapman et al., 2002). Fish embryos of *Austrofundulus limnaeus* are surrounded by an egg envelope composed of two proteins that together form a structure similar to amyloid fibrils. This amyloid chorion protects the fish embryo from mechanical disruption, serves as a barrier to polyspermy, microbes, and low molecular weight solutes, and is able to help prevent dehydration of the embryo by preventing water loss (Podrabsky et al., 2001). It is possible that a conformational change of type I AFP at physiological concentrations may play a role in ice inhibition. Indeed, the insect antifreeze proteins have a parallel β-helix structure (Graether et al., 2000; Liou et al., 2000), a motif that has been shown to bind Congo Red (Khurana et al., 2001). Possibly the remarkable properties of AFP (such as alignment of proteins on the ice surface) promote the ordered aggregation of neighboring molecules into the parallel β-sheet structure, that, under high concentrations, can form amyloid. We are currently investigating

how this may be involved in AFP function and fibril formation.

Amyloidogenesis and applications of AFPs

The type I AFP is found in the circulatory system of fish at a concentration of 10-15 mg/mL (Fletcher et al., 2001). The relatively low physiological concentration of the protein and its ability to bind to membranes (Tomczak et al., 2002) may prevent it from self-association. However, there is a question concerning the freezing of fish for long-term storage, and whether other potentially fibril-forming proteins could similarly form amyloid-like fibrils upon freezing and thawing. Inasmuch as type I AFP can form amyloid, its use in applications (Fletcher et al., 1999) such as cryo-preservation, cryosurgery, as a food additive, and in expression in transgenic organisms needs to be addressed (Crevel et al., 2002).

REFERENCES

Balbach, J. J., Y. Ishii, O. N. Antzutkin, R. D. Leapman, N. W. Rizzo, F. Dyda, J. Reed, and R. Tycko. 2000. Amyloid fibril formation by A beta(16–22), a seven-residue fragment of the Alzheimer's beta-amyloid peptide, and structural characterization by solid-state NMR. *Biochemistry.* 39:13748–13759.

Balbach, J. J., A. T. Petkova, N. A. Oyler, O. N. Antzutkin, D. J. Gordon, S. C. Meredith, and R. Tycko. 2002. Supramolecular structure in full-length Alzheimer's beta-amyloid fibrils: evidence for a parallel beta-sheet organization from solid-state nuclear magnetic resonance. *Biophys. J.* 83:1205–1216.

Benzinger, T. L., D. M. Gregory, T. S. Burkoth, H. Miller-Auer, D. G. Lynn, R. E. Botto, and S. C. Meredith. 2000. Two-dimensional structure of beta-amyloid(10–35) fibrils. *Biochemistry.* 39:3491–3499.

Bucciantini, M., E. Giannoni, F. Chiti, F. Baroni, L. Formigli, J. Zurdo, N. Taddei, G. Ramponi, C. M. Dobson, and M. Stefani. 2002. Inherent toxicity of aggregates implies a common mechanism for protein misfolding diseases. *Nature.* 416:507–511.

Chapman, M. R., L. S. Robinson, J. S. Pinkner, R. Roth, J. Heuser, M. Hammar, S. Normark, and S. J. Hultgren. 2002. Role of *Escherichia coli* Curli operons in directing amyloid fiber formation. *Science.* 295:851–855.

Chiti, F., M. Bucciantini, C. Capanni, N. Taddei, C. M. Dobson, and M. Stefani. 2001. Solution conditions can promote formation of either amyloid protofilaments or mature fibrils from the HypF N-terminal domain. *Prot. Sci.* 10:2541–2547.

Chiti, F., N. Taddei, M. Bucciantini, P. White, G. Ramponi, and C. M. Dobson. 2000. Mutational analysis of the propensity for amyloid formation by a globular protein. *EMBO J.* 19:1441–1449.

Chiti, F., P. Webster, N. Taddei, A. Clark, M. Stefani, G. Ramponi, and C. M. Dobson. 1999. Designing conditions for in vitro formation of amyloid protofilaments and fibrils. *Proc. Natl. Acad. Sci. USA.* 96:3590–3594.

Costa, P. R., D. A. Kocisko, B. Q. Sun, P. T. Lansbury, and R. G. Griffin. 1997. Determination of peptide amide configuration in a model amyloid fibril by solid-state NMR. *J. Am. Chem. Soc.* 119:10487–10493.

Crevel, R. W., J. K. Fedyk, and M. J. Spurgeon. 2002. Antifreeze proteins: characteristics, occurrence and human exposure. *Food Chem. Toxicol.* 40:899–903.

Dobson, C. M. 1999. Protein misfolding, evolution and disease. *Trends Biochem. Sci.* 24:329–332.

Dobson, C. M. 2001. The structural basis of protein folding and its links with human disease. *Phil. Trans. R. Soc. Lond. B.* 356:133–145.

Fandrich, M., M. A. Fletcher, and C. M. Dobson. 2001. Amyloid fibrils from muscle myoglobin. *Nature.* 410:165–166.

Fezoui, Y., D. M. Hartley, D. M. Walsh, D. J. Selkoe, J. J. Osterhout, and D. B. Teplow. 2000. A de novo designed helix-turn-helix peptide forms nontoxic amyloid fibrils. *Nat. Struct. Biol.* 7:1095–1099.

Fletcher, G. L., S. V. Goddard, and Y. Wu. 1999. Antifreeze proteins and their genes: From basic research to business opportunities. *Chemtech.* 30:17–28.

Fletcher, G. L., C. L. Hew, and P. L. Davies. 2001. Antifreeze proteins of Teleost fishes. *Annu. Rev. Physiol.* 63:359–390.

Graether, S. P., M. J. Kuiper, S. M. Gagné, V. K. Walker, Z. Jia, B. D. Sykes, and P. L. Davies. 2000. β-helix structure and ice-binding properties of a hyperactive antifreeze protein from an insect. *Nature.* 406:325–328.

Graether, S. P., C. M. Slupsky, P. L. Davies, and B. D. Sykes. 2001. Structure of type I antifreeze protein and mutants in supercooled water. *Biophys. J.* 81:1677–1683.

Gross, M., D. K. Wilkins, M. C. Pitkeathly, E. W. Chung, C. Higham, A. Clark, and C. M. Dobson. 1999. Formation of amyloid fibrils by peptides derived from the bacterial cold shock protein CspB. *Protein Sci.* 8:1350–1357.

Guijarro, J. I., M. Sunde, J. A. Jones, I. D. Campbell, and C. M. Dobson. 1998. Amyloid fibril formation by an SH3 domain. *Proc. Natl. Acad. Sci. USA.* 95:4224–4228.

Harper, J. D., and P. T. Lansbury. 1997. Models of amyloid seeding in Alzheimer's disease and scrapie: mechanistic truths and physiological consequences of the time-dependent solubility of amyloid proteins. *Annu. Rev. Biochem.* 66:385–407.

Hodges, R. S., P. D. Semchuk, A. K. Taneja, C. M. Kay, J. M. Parker, and C. T. Mant. 1988. Protein design using model synthetic peptides. *J. Pept. Res.* 1:19–30.

Jia, Z., and P. L. Davies. 2002. Antifreeze proteins: an unusual receptor-ligand interaction. *Trends Biochem. Sci.* 27:101–106.

Kelly, J. W. 1998. The alternative conformations of amyloidogenic proteins and their multi-step assembly pathways. *Curr. Opin. Struct. Biol.* 8:101–106.

Khurana, R., V. N. Uversky, L. Nielsen, and A. L. Fink. 2001. Is Congo Red an amyloid-specific dye? *J. Biol. Chem.* 276:22715–22721.

Kisilevsky, R. 2000. Review: Amyloidogenesis—unquestioned answers and unanswered questions. *J. Struct. Biol.* 130:99–108.

Laws, D. D., H. M. L. Bitter, K. Liu, H. L. Ball, K. Kaneko, H. Wille, F. E. Cohen, S. B. Prusiner, A. Pines, and D. E. Wemmer. 2001. Solid-state NMR studies of the secondary structure of a mutant prion protein fragment of 55 residues that induces neurodegeneration. *Proc. Natl. Acad. Sci. USA.* 98:11686–11690.

LeVine, H. 1999. Quantification of β-sheet amyloid fibril structures with Thioflavin, T. *Meth. Enzymol.* 309:274–284.

Liou, Y., A. Tocilj, P. L. Davies, and Z. Jia. 2000. Mimicry of ice structure by surface hydroxyls and water of a β-helix antifreeze protein. *Nature.* 406:322–324.

Litvinovich, S. V., S. A. Brew, S. Aota, S. K. Akiyama, C. Haudenschild, and K. C. Ingham. 1998. Formation of amyloid-like fibrils by self-association of a partially unfolded fibronectin type III module. *J. Mol. Biol.* 280:245–258.

Pepys, M. B. 2001. Pathogenesis, diagnosis and treatment of systemic amyloidosis. *Philos. Trans. R. Soc. Lond. B Biol. Sci.* 356:203–210.

Podrabsky, J. E., J. F. Carpenter, and S. C. Hand. 2001. Survival of water stress in annual fish embryos: Dehydration aviodance and egg envelope amyloid fibers. *Am. J. Physiol. Regulatory Integrative Comp. Physiol.* 280:R123–R131.

Puchtler, H., F. Sweat, and M. Levine. 1962. On the binding of Congo Red by amyloid. *J. Histochem. Cytochem.* 10:355–364.

Serpell, L. C., M. Sunde, and C. C. F. Blake. 1997. The molecular basis of amyloidosis. *Cell. Mol. Life Sci.* 53:871–887.

Sicheri, F., and D. S. Yang. 1995. Ice-binding structure and mechanism of an antifreeze protein from winter flounder. *Nature.* 375:427–431.

Spencer, R. G. S., K. J. Halverson, M. Auger, A. E. McDermott, R. G. Griffin, and P. T. Lansbury. 1991. An unusual peptide conformation may precipitate amyloid formation in Alzheimers disease: application of solid-state NMR to the determination of protein secondary structure. *Biochemistry.* 30:10382–10387.

Tomczak, M. M., D. K. Hincha, S. D. Estrada, W. F. Wolkers, L. M. Crowe, R. E. Feeney, F. Tablin, and J. H. Crowe. 2002. A mechanism for stabilization of membranes at low temperatures by an antifreeze protein. *Biophys. J.* 82:874–881.

Wishart, D. S., C. G. Bigam, J. Yao, F. Abildgaard, H. J. Dyson, E. Oldfield, J. L. Markley, and B. D. Sykes. 1995. ^{1}H, ^{13}C and ^{15}N chemical shift referencing in biomolecular NMR. *J. Biomol. NMR.* 6:135–140.

Wishart, D. S., R. F. Boyko, L. Willard, F. M. Richards, and B. D. Sykes. 1994. SEQSEE: a comprehensive program suite for protein sequence analysis. *Comp. Appl. Biosci.* 10:121–132.

The behaviour of polyamino acids reveals an inverse side chain effect in amyloid structure formation

Marcus Fändrich[1,2] and Christopher M.Dobson[3]

Oxford Centre for Molecular Sciences, Central Chemistry Laboratory, University of Oxford, South Parks Road, Oxford OX1 3QT, UK

[1]Present address: Institut für Molekulare Biotechnologie (IMB), Beutenbergstraße 11, Postfach 100 813, D-07708 Jena, Germany
[3]Present address: Department of Chemistry, University of Cambridge, Lensfield Road, Cambridge CB2 1EW, UK

[2]Corresponding author
e-mail: fandrich@imb-jena.de

Amyloid fibrils and prions are proteinaceous aggregates that are based on a unique form of polypeptide configuration, termed cross-β structure. Using a group of chemically distinct polyamino acids, we show here that the existence of such a structure does not require the presence of specific side chain interactions or sequence patterns. These observations firmly establish that amyloid formation and protein folding represent two fundamentally different ways of organizing polypeptides into ordered conformations. Protein folding depends critically on the presence of distinctive side chain sequences and produces a unique globular fold. By contrast, the properties of different polyamino acids suggest that amyloid formation arises primarily from main chain interactions that are, in some environments, overruled by specific side chain contacts. This side chain effect can be thought of as the inverse of the one that characterizes protein folding. Conditions including Alzheimer's and Creutzfeldt–Jakob diseases represent, on this basis, pathological cases in which a natural polypeptide chain has aberrantly adopted the conformation that is primarily defined by main chain interactions and not the structure that is determined by specific side chain contacts that depend on the polypeptide sequence.
Keywords: aggregation/amyloid fibril/inverse side chain effect/polyamino acid/protein folding

Introduction

A group of highly debilitating conditions, including Alzheimer's, Creutzfeldt–Jakob, Huntington's and Parkinson's diseases, are characterized by the deposition of proteinaceous aggregates, including amyloid fibrils and prions (Sunde and Blake, 1998; Dobson, 2001). These aggregates involve a specific type of polypeptide conformation, termed 'cross-β structure'. This conformational state consists of intermolecular β-sheets in a distinctive orientation such that the strands from which these sheets are assembled extend transversely to the major axis of the fibril (Sunde and Blake, 1998). More than 20 natural polypeptides have been found to produce amyloid fibrils inside living organisms in an aberrant manner and thereby to give rise to disease (Sunde and Blake, 1998). In the case of prions, aggregates with cross-β structure can serve as templates that transmit specific steric information to another organism, thus propagating as stable molecular and clinical strains (Prusiner, 1998). It has remained unclear, however, to what extent our present understanding of protein structure might suffice to describe the formation of the particular polypeptide conformations that are specific for the formation of the amyloid core structure.

According to protein folding theory, the side chain sequence encodes the way in which a natural polypeptide chain folds up into a globular structure (Anfinsen, 1973; Dill *et al.*, 1995; Dobson *et al.*, 1998; Baker, 2000). On this basis, a given polypeptide chain is able to give rise to a single ordered conformation. In a similar manner, the existence of amyloid structures has been associated with some specific (albeit generally unrelated) sequence properties, such as the presence of side chain amide groups (Perutz *et al.*, 1994; DePace *et al.*, 1998), certain binary patterns (West *et al.*, 1999; Rochet and Lansbury, 2000) or secondary structural propensities (Rochet and Lansbury, 2000). In contrast, we found that myoglobin, the textbook example of an α-helical and globular protein structure is able to adopt a conformation that is fundamentally different from the native state and shows the typical characteristics of pathological amyloid fibrils (Fändrich *et al.*, 2001). Moreover, observations that numerous polypeptides can adopt amyloid structure under appropriate conditions *in vitro*, although these are not known to relate to any misfolding disease, have suggested that many, perhaps all, polypeptide chains are able to form amyloid fibrils (Chiti *et al.*, 1999; Dobson, 1999, 2001; Fändrich *et al.*, 2001). However, it follows from such proposals that specific sequences, despite their very significant influence on the rates and conditions under which such aggregates form (Dobson, 2001; Chiti *et al.*, 2002), are not required. Using polyamino acids (PAAs), we set out to resolve these apparently paradoxical observations concerning the effect of the side chain sequence and to assess the relationship between amyloid formation and protein folding. PAAs are simple polypeptide model systems that lack a distinctive sequence and hence also the ability to fold. Their high molecular weight enables the study of the invariant polypeptide properties under conditions in which the effects of the chain ends are negligible.

Results and discussion

Polyamino acids can form fibrillar aggregates
PAAs have long been known to adopt different configurations depending on the physico-chemical environment in
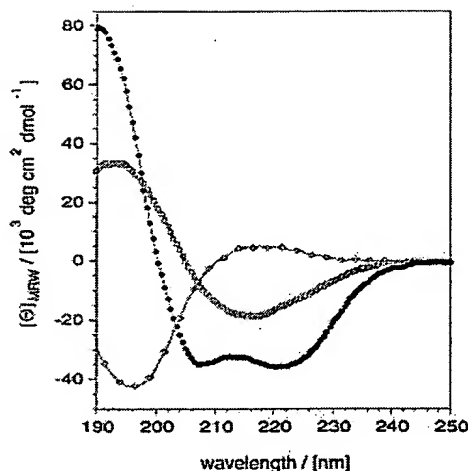
Fig. 1. Far-UV CD spectra of different conformations of poly-L-lysine. The far-UV CD spectra of 0.1 mg/ml poly-L-lysine in an α-helical (filled circles, freshly dissolved PK at pH 11.1), β-sheet (open circles, PK at pH 11.1 after heating for 15 min, 52°C) and random coil conformation (diamonds, freshly dissolved PK in pure water).

Fig. 2. Morphology of PAA fibrils defined by EM. PK: (A) 2.5 mg/ml, H_2O, pH 11.2, 65°C, 4 days or (B) 1 mg/ml, H_2O, pH 10.1, 65°C, 1 week. Arrowheads emphasize the constrictions of a ribbon-like morphology. PE: (C) 1 mg/ml, D_2O, pD 4.08, 65°C, 2 days or (D) H_2O, pH 4.1, 65°C, 6 days. PT: 10 mg/ml (E and F) or 1 mg/ml (G) PT in 50 mM sodium borate pH 9.0 was exposed for 4 days to 65°C. Samples in (E) and (F) subsequently were kept at room temperature for 6 weeks. Scale bars: 200 nm (white), 100 nm (black).

which they are found. One example is the structural variability of poly-L-lysine (PK) that is revealed clearly by using circular dichroism (CD) spectroscopy (Figure 1). PK is disordered in water at pH 7 but collapses readily into an α-helical structure if the pH is increased to 11.1. In contrast, heating at this high pH value irreversibly converts α-helical PK into a β-form (Greenfield et al., 1969). When we placed solutions containing β-PK at room temperature and monitored its conformation by CD, β-PK was not found to revert into α-PK within the time span investigated (up to 1 week). However, readjusting the pH from 11.1 to a near neutral value led to the immediate conversion of β-PK into a random coil state, as seen by CD. The characteristics of β-PK and the similarity of some of these procedures to protocols for the conversion of globular proteins, such as the α-helical myoglobin, into amyloid fibrils (Fändrich et al., 2001) prompted us to examine the ultrastructural organization of β-PK by electron microscopy (EM).

We found that heating at pH 11.1 readily induces the formation of large quantities of fibrillar aggregates (Figure 2A and B). These structures can be seen to be up to 11 nm wide and of a variable length (Figure 2A). Occasionally, we observe ribbon-like morphologies with a helical pitch of ~100 nm (Figure 2B). We have found that other water-soluble PAAs can produce similar species by careful choice of conditions. For example, poly-L-glutamic acid (PE) was observed to form fibrils at pH values close to 4 (Figure 2C and D). Compared with the other PAAs, some PE aggregates appear less well organized, presumably because the high propensity to precipitate rapidly precludes the formation of highly ordered aggregates in saturated PE solutions. Increasing the pH value to near neutral values led to the dissociation of these PE aggregates. In contrast, the aggregates formed by the more soluble poly-L-threonine (PT) at pH 9 are better delineated and defined. Different morphologies can,
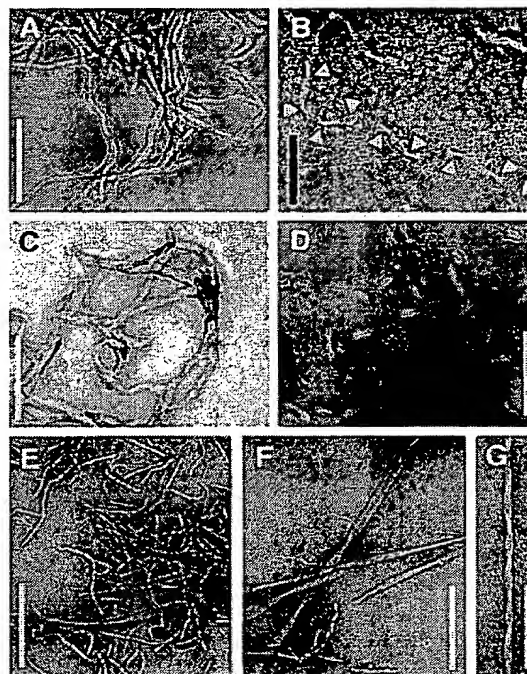
however, be discerned (Figure 2E–G). We encountered thin filaments (diameter <5 nm), tapes (diameter 8–9 nm) with lengths of up to 200 nm, as well as highly ordered fibrils. The latter are generally longer than 1 μm (Figure 2F and G) and often occurred in the form of broad plates with diameters up to 70 nm or helical bundles with diameters of 20 nm and a pitch of ~170 nm. Fibrillar structures (in particular the highly ordered PT fibrils) were found to form only after prolonged incubation (>1 day) and by rearrangement from an aggregated but less well organized (by EM) precursor that can already be detected (by IR spectroscopy) at much shorter incubation times (<15 min). In contrast to PK and PE, PT did not require heating to promote aggregation. The species observed correspond in their overall appearance to the morphologies of amyloid aggregates formed from peptides and proteins, including those associated with specific diseases (Sunde and Blake, 1998).

We have, in addition, examined several hydrophobic PAAs including the polymers of alanine, valine, lecuine, isoleucine, phenylalanine and tyrosine. We found that the commercially available polymers of very high molecular weight were extremely prone to undergo precipitation reactions, thus preventing the study of aggregate formation. Some dissolved in concentrated trifluoroacetic acid (TFA) or dichloroacetic acid, but they precipitated effectively instantaneously upon addition of small quantities of
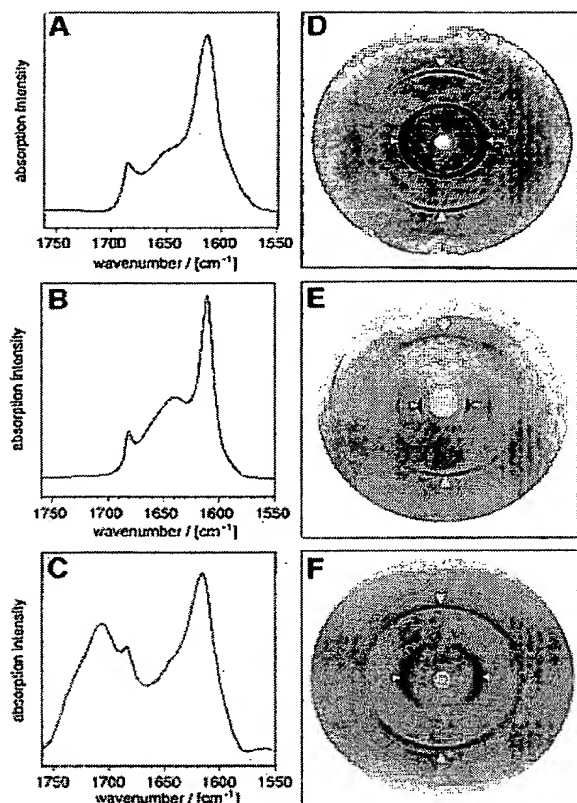
Fig. 3. Internal conformations of fibrillar PAAs. FTIR amide I' region of PT (A), PK (B) and PE (C) in D_2O. Maxima: 1614 and 1685/cm (A); 1611 and 1680/cm (B); and 1616, 1683 and 1706/cm (C). X-ray diffraction pictures of films cast from PT (D), PK (E) and PE (F). To obtain the β-form of PE, the PAA was dissolved at 25 mg/ml in D_2O, pD 4.1 and heated for 4 h to 95°C. Arrowheads are parallel to the plane of the film and show the main chain spacing; the arrows point to the side chain spacing.

aqueous solutions, acetonitrile or methanol. However, early studies using organic solvents have already demonstrated that several of these PAAs can readily aggregate into β-structures under specific conditions or as small peptides (Arnott et al., 1967; Glenner et al., 1972; Komoto et al., 1974; Lotz, 1974). Interestingly, we found that the dimensions reported for these aggregated structures correspond closely to those of disease-related amyloid fibrils or the aggregates of water-soluble PAAs (see below).

Fibrillar PAA aggregates possess the characteristics of amyloid structures

In order to assess whether or not these fibrils show the characteristic polypeptide chain arrangement of aggregated β-sheet structures, we examined them by Fourier transform infrared (FTIR) spectroscopy. The spectra obtained showed that the three PAAs produce very similar amide I' regions (Figure 3A–C) that contained absorption maxima at 1611 cm⁻¹ for PK, 1616 cm⁻¹ for PE and 1614 cm⁻¹ for PT, demonstrating the presence of aggregated β-sheets. Using X-ray diffraction techniques, we

Table I. Observed Bragg spacings of β-PAAs (in Å)

PE	PK	PT	PE + PK
4.73 m	4.67 m	4.77 m	4.67
3.87 m	3.79 m	3.62 m	3.74
9.6 e	14.6 e	8.77 e	13.7
	7.5 e		6.9
	5.0 e		

m, meridional reflection; e, equatorial reflection.

then tested whether these β-sheets possess the orientation properties characteristic of amyloid fibrils. These methods provide the most specific and direct test for the presence of a cross-β structure; if fibrils containing such structure are aligned and oriented with their main axes perpendicular to the X-ray beam, a highly characteristic diffraction pattern can be observed. At least two reflections must be present in this pattern to be defined as cross-β structure: a sharp meridional one at almost precisely 4.75 Å corresponding to the separation of two hydrogen-bonded chains (the 'main chain reflection') and an equatorial one that is more variable and that is often seen to be close to 10 Å (Sunde et al., 1997). This so-called 'side chain reflection' depends on the packing distance between two juxtaposed β-sheets. The typical anisotropy of the diffraction patterns of amyloid fibrils implies a β-sheet orientation in which the hydrogen bonds and the plane of the sheet are parallel to the main fibril axis, whereas backbone and side chains extend transversely to this axis.

Alignment of the PAA fibrils was achieved by drying aliquots of the sample solution onto a glass slide (Perutz et al., 1994). When films cast from such materials were exposed to X-rays in such a way that the plane of the film was mounted parallel to the beam, diffraction patterns of the typical cross-β type could be observed (Figure 3D–F). The orientation of the main chain and side chain spacings, together with their breadth ratio, demonstrates an organization of β-crystallites in a fibrillar arrangement characteristic of amyloid structure. On the meridian, two reflections were conserved in all patterns (Table I). These were close to 4.7 Å (the main chain spacing) and 3.7 Å. Both diffraction spots are encountered commonly in the patterns of amyloid fibrils (Sunde et al., 1997), and the clear conservation of the main chain spacing reflects the invariant backbone geometry of β-sheets. In contrast, the value of the side chain spacing varied considerably between different PAAs and ranged from 8.77 Å (PT) and 9.6 Å (PE) to 14.6 Å (PK) (see Table I). Consistent with its association with intersheet distances, we find that this spacing correlates closely with the van der Waals volumes of the amino acid residue concerned (Figure 4). In addition, Figure 4 shows that our measurements on fibrillar PAAs are in excellent agreement with the dimensions reported in some very early studies for the β-structure of PAA aggregates (Arnott et al., 1967; Glenner et al., 1972; Komoto et al., 1974; Lotz, 1974). Moreover, if we compare the side chain spacings of amyloid fibrils from peptides having a heterogeneous sequence with their average residual volume, we observe, despite a greater scatter, the same type of correlation as for PAAs (Figure 4).

These findings provide strong support for previous ideas in which the fundamental polypeptide arrangement of
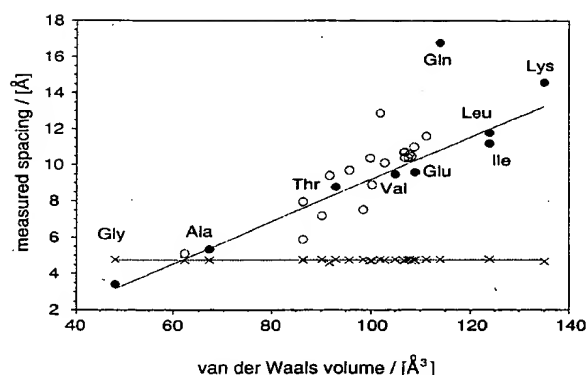
Fig. 4. Comparison of the internal structure of PAA fibrils and other amyloid structures. Correlation of the main chain spacing (crosses) and the side chain spacing (circles) with the residual volume (Creighton, 1993). Closed symbols, PAAs (Arnott *et al.*, 1967; Komoto *et al.*, 1974; Lotz, 1974; Perutz *et al.*, 1994); open symbols, heterogeneous sequences (Glenner *et al.*, 1974; Inouye *et al.*, 1993, 2000; Nguyen *et al.*, 1995; Weaver, *et al.*, 1996; Symmons *et al.*, 1997; Kirschner *et al.*, 1998; Malinchik *et al.*, 1998; Groß *et al.*, 1999; Luckey *et al.*, 2000; Serpell *et al.*, 2000). A linear fit to the PAA side chain spacings (excluding glutamine) is shown.

amyloid fibrils has been represented as a cross-β structure (Sunde and Blake, 1998). Moreover, the quantitative manner of the correlation described here is particularly interesting as it may provide a means to assess the nature of the sequence regions within natural proteins from which the core structure of amyloid fibrils is formed. Of the various PAAs, only the proposed overall structure of poly-L-glutamine aggregates deviates significantly from this relationship. The published intersheet distance of poly-L-glutamine aggregates (16.8 Å) clearly exceeds the value expected from the dimensions of glutamine side chains (see Figure 4). The reasons for these deviations remain to be established, but intercalation of other species, hydration effects or specific alterations in the overall aggregate structure are possible explanations (Perutz *et al.*, 2002). The fibrillar PAA aggregates that we have examined in this study, however, are based on the same fundamental type of structure as those amyloid fibrils that are constructed from heterogeneous sequences and that are associated with clinical conditions.

Amyloid formation and protein folding are distinct processes

Amyloid formation has often been described as an aberrant pathway within protein folding reactions that diverges from the routes leading to the native state after some initial folding events have produced a partially folded intermediate state. Although this description might well reflect, for some polypeptide systems, the order of events that can be observed experimentally within the particular physico-chemical environment chosen for analysis, we believe that amyloid formation differs from protein folding in a more radical way than has been generally recognized. Protein folding depends critically on a distinctive sequence and produces a globular structure that is specific for the respective polypeptide sequence (Anfinsen, 1973; Dill *et al.*, 1995; Dobson *et al.*, 1998; Baker, 2000). In contrast,

PAAs do not possess any specific sequence and are, for this reason, intrinsically unable to fold to specific globular structures (Dill *et al.*, 1995). Our observation that different PAAs are able to form amyloid structures nevertheless demonstrates that this configuration is not the product of a protein folding reaction and represents, instead, a generic type of chain arrangement that is defined by interactions that are common to different sequences, in particular those involving the main chain (Fändrich *et al.*, 2001). Although the nature of, and interactions between, the side chains of the polypeptide involved will influence the stability of the amyloid state relative to others including the folded state, and indeed can influence the details of the fibrillar assembly, they do not dictate the fundamental organisation of the cross-β structure. Amyloid formation does not therefore relate to protein folding, and represents, instead, an entirely different and unique way of organizing the polypeptide chain into an ordered conformation.

Polypeptides are organic polymers that are constructed from units containing the same basic structure, that of an α-amino acid. Natural polypeptides, however, are highly selected sequences and contrast to many of the synthetic polymers in the remarkable structural and chemical diversity that is manifested in their side chains and which has conferred on them the ability to fold into proteins, i.e. to adopt highly specific and globular states. Nevertheless, we believe that natural polypeptides can adopt, in addition to their specific globular protein conformation, a generic structure that reflects their character as organic polymers. This structure is the one that is seen in amyloid fibrils. Three observations provide strong support to this concept. First, amyloid structures are not inherently the product of specific side chain interactions. The PAAs used in this study vary in the structure and properties of their side chains, including such features as their secondary structure propensities, hydrophobicity and electrostatic properties. Most notably, they all lack asparagine and glutamine residues, demonstrating that, despite their frequent occurrence in clinical polypeptide aggregates (Perutz *et al.*, 1994; DePace *et al.*, 1998), these specific residues and their associated properties are not necessary for amyloid formation. Secondly, mutations that alter the main chain properties, such as proline insertions, are found generally to perturb amyloid formation (Moriarty and Raleigh, 1999; Wigley *et al.*, 2002). Thirdly, some synthetic polymers (polyamides or nylons) which lack side chains are known to adopt a chain arrangement similar to the aggregated polypeptide states discussed here (Bunn and Garner, 1947). Although polyamides have different energetic properties compared with polypeptides, both organic polymer chains possess a similar molecular structure.

The kinetic partitioning between aggregates and alternative conformations

Despite the generic nature of the amyloid structure, different polypeptide chains can differ considerably in their aggregation behaviour within the same physico-chemical environment. Moreover, PAAs require, as do other polypeptides, distinctive conditions in order to form amyloid aggregates. We have therefore utilized our set of PAAs to explore the effects of several physico-chemical parameters on the aggregation reaction and to assess, more
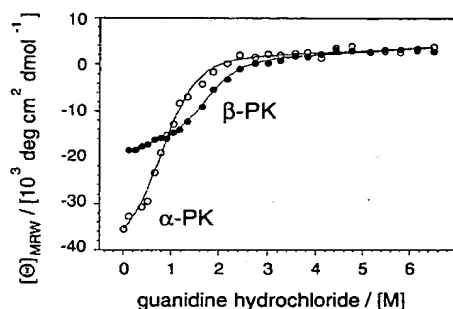
5685

Fig. 5. Stability of α-PK and β-PK against denaturation. Guanidine hydrochloride denaturation of α-PK (222 nm, open symbols) and β-PK (217 nm, closed symbols) monitored by CD and fitted to a two-state transition (Santoro and Bolen, 1988).

generally, the relationship between the common and the specific properties of different polypeptide chains. For example, the aggregation reactions of α-helical PK, PE and poly-L-alanine (Blondelle et al., 1997) are accelerated by heating. This α to β transition is macroscopically irreversible, i.e. if these PAA solutions are placed at room temperature the aggregated chains will not revert spontaneously to an α-helical species. In fact, β-PK is, at room temperature, even more resistant to chaotropic denaturation using guanidine hydrochloride (transition midpoint 1.76 M) than the α-helical form (0.77 M), as shown in Figure 5. Yet, the α-helical configuration forms most readily under these conditions, suggesting that the formation of this structure is due to a kinetic rather than a thermodynamic preference. In contrast to these clear effects on the polypeptide conformation, we could not obtain any evidence that heating promotes the formation of any covalent modifications. All three PAAs were incubated in their respective buffers for up to 4 weeks at 65°C and examined by amino acid analysis. On the basis of their UV profiles in reversed phase chromatography, no samples used in this study contained significant quantities of covalently modified residues, even after this prolonged heating.

From these data, we conclude that the partitioning of these PAAs between the α-helical and the amyloid form is critically determined by the stability of the α-helical form. In an environment that supports the conformational stability of this state, α-helices can prevent the polypeptide chain from converting into amyloid structures. These findings on PAAs resemble closely the case of proteins such as myoglobin that form amyloid fibrils at elevated temperatures where the globular structure is disrupted (Fändrich et al., 2001). Taken together, we believe that the presence of an α-helical or globular conformations represents one way, amongst others (Richardson and Richardson, 2002), to suppress amyloid formation by making the polypeptide backbone inaccessible for intermolecular interactions. Further support for this view comes from the observations that PT, poly-L-asparagine and poly-L-glutamine, residues with lower α-helical propensities such that PAAs do not adopt stable α-helical structures in water, form amyloid structures at room temperature (Perutz et al., 2002). Under conditions in

which α-helices or globular proteins are unstable, the main chain of a polypeptide will become disordered, solvent exposed and prone to aggregate.

These schemes imply that α-helical or globular polypeptide conformations are able to form faster than amyloid structures. By analogy to globular proteins, in which fast folding correlates with a high proportion of short-range interactions (Baker, 2000), we believe that a kinetic preference for α-helical or globular species is plausible on the basis of the higher proportion of short-range interactions stabilizing these conformations compared with the intermolecular β-sheet structure of aggregates. These ideas are supported further by findings that the formation of the cellular α-helical isoform of the prion protein is under kinetic control (Baskakov et al., 2000) as well as observations that high α-helical propensities can suppress amyloid formation (Villegas et al., 2000). The very fast precipitation reactions of hydrophobic PAAs discussed above and the common insolubility of polypeptides at their isoelectric points (Zurdo et al., 2001) represent further examples of reaction pathways that compete with, and are able to block, amyloid formation.

An inverse side chain effect governs amyloid formation by polyamino acids

The simple presence of a disordered polypeptide chain does not, however, generally suffice for aggregation. Neither PK nor PE aggregates in pure water at a pH near to neutral; under these conditions, unfavourable coulombic interactions between the side chains will make both α-helical and aggregated β-structures unfavourable (Figure 6A and B). In contrast, it has been shown previously that specific counterions that compensate for these electrostatic effects promote the aggregation of these PAAs. X-ray analysis of these aggregates reveals intersheet spacings larger than those observed in the present analysis. For example, the intersheet distance of PE increases from 9.6 to 12.6 Å in the presence of Ca^{2+} (Keith et al., 1969) and, in the case of PK solutions containing HPO_4^{2-} ions, from 14.6 to 17.0 Å (Padden et al., 1969). The larger values of side chain spacings suggest an intercalation of these counterions between otherwise densely packed β-sheets. Hence, the side chain interactions across these sheets must be diminished. Uncompensated electrostatic groups therefore represent one example of a specific side chain contact that can depend on the physicochemical environment and that can repress amyloid formation by destabilizing the amyloid core structure.

Based on these observations, we speculated that complementary charged side chains might mutually suppress the unfavourable electrostatic properties of the isolated chains by forming mixed aggregates. Indeed, when a 1:1 mixture of PK and PE was exposed to conditions that do not promote the aggregation of either PAA in isolation, namely in aqueous solution at near neutral pH and at room temperature, large quantities of aggregates were found to form (Figure 6C). Although well-defined fibrils were not detected in such experiments by EM, presumably as a result of the insolubility of these species and their strong propensity to precipitate, X-ray diffraction analysis reveals an intersheet distance of 13.7 Å (Table I). This value differs from the side chain spacings of PK (14.6 Å) and PE (9.6 Å) aggregates, and is also
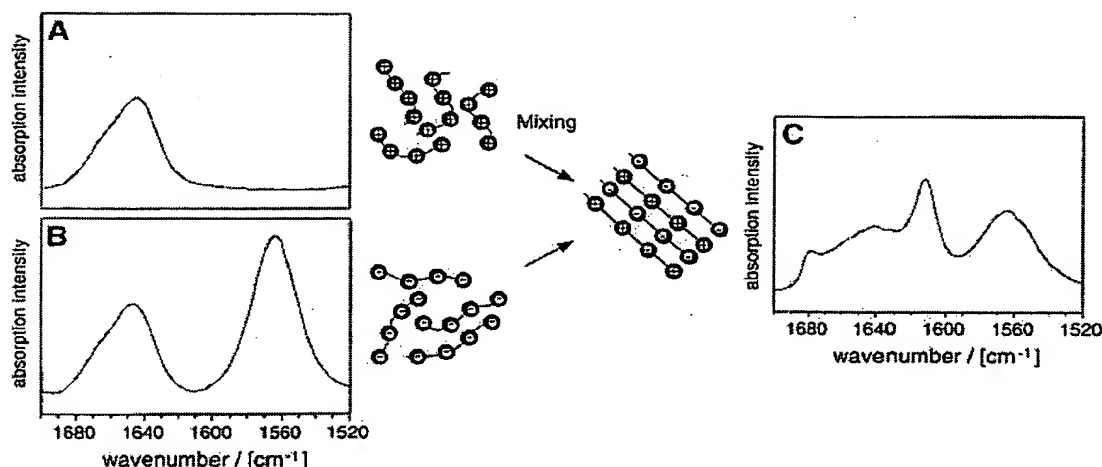
Fig. 6. Formation of mixed aggregates from PE and PK. PK (A) and PE (B) do not aggregate in D_2O, pD 7.5. The FTIR spectra show a random coil structure. On mixing the two solutions, the PE and PK aggregates are formed (C). FTIR spectra were recorded in D_2O, pD 7.5. The total free amino acid concentrations were all 0.1 M. Amide I′ maxima: 1646 cm^{-1} (PE and PK in isolation); 1612, 1679 and 1642 cm^{-1} (mixed aggregates). The carboxylate group gives rise to a peak at 1565 cm^{-1}.
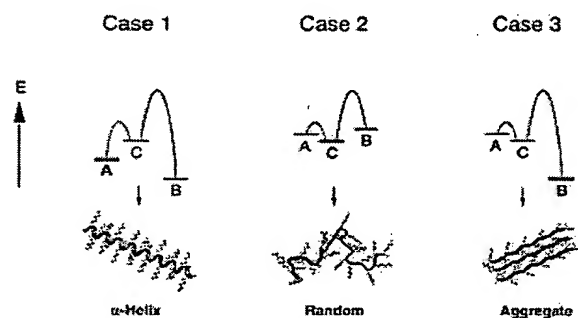

Fig. 7. The partitioning between folding and amyloid formation. Polypeptides that can adopt ordered states with low contact order (A or α-PK), an ordered state with high contact order (B or β-PK) and a random coil state (C) show different relative energies under different physico-chemical conditions (cases 1–3). For example, the PK side chains have properties that destabilize both states A and B at neutral pH (case 2). Upon increasing the pH, unfavourable electrostatic effects are reduced. Since A is kinetically favourable over B (case 1), the latter state can only be observed under conditions that destabilize A, such as mild heating (case 3).

larger than their average (12.1 Å), suggesting that lysine residues are present in all these densely packed sheets and that the two PAAs form mixed aggregates. These observations not only support the idea of a generic polypeptide structure, but they are also in accord with our proposals concerning the influence of charged side chains on aggregation reactions.

Figure 7 illustrates schematically the possible thermodynamic relationship between the three distinct conformational states of PK (here abbreviated as A, B and C). State C corresponds to a random coil structure, and states A and B represent two ordered conformations. We assume that A (here the α-helical conformation) contains many

more local contacts than B (corresponding to amyloid structures). By analogy with a computational analysis of the kinetic partitioning between different folded conformations in a cubic-lattice system (Abkevich et al., 1998), the energy barriers of the formation of A from the unstructured state C will be lower than for the reaction from C to B. The relative energies of the three states and their interconnecting transition states will be determined, for a given polypeptide chain such as PK, by the physico-chemical environment. Although temperature will also affect the height of the energy barrier of the different transition states, aggregation will depend mainly on the extent to which the conditions make potentially competing states of lower contact order unfavourable (Figure 7, case 3).

It follows from these ideas that the side chains influence, in these cases, amyloid formation in a manner that contrasts radically with their effect on the process of protein folding. Protein folding reactions depend on a productive side chain effect, i.e. the polypeptide sequence determines the structure of the reaction product (Anfinsen, 1973; Dill et al., 1995; Dobson et al., 1998; Baker, 2000). A similar assumption, namely that polypeptides cannot convert into amyloid structures unless specific sequences encode this state, has been implied by many previous hypotheses concerning amyloid formation. We believe, however, that our present data demonstrate, at least for the PAAs used in this study, an effect of the side chains that is effectively the inverse of such proposals, namely that the common ability of polypeptide chains to aggregate is, in some circumstances, overruled by specific side chain interactions. Such a suppressive effect is exerted either by destabilizing aggregated structures or by promoting alternative states that are kinetically favourable compared with amyloid formation. Stable α-helical structures or cooperative globular protein conformations represent examples of such alternative states. Destabilization of the interactions that disfavour amyloid structure, for example by changing the experimental conditions, can result in a

higher population of disordered chains that are competent to convert into fibrillar states. Once formed, these states resist ready dissociation, largely as a result of substantive transition state barriers or desolvation. The various PAAs differ therefore in their apparent 'amyloidogenicity', and the general observation that any polypeptide chain requires particular physico-chemical conditions to promote fibril formation also reflects the fact that not all solution conditions inhibit amyloid formation to the same extent. It is of note that polyglycine and polyamides might therefore be expected to form this structure very readily. Indeed, these polymers have been found to form such fibrillar aggregates (Bunn and Garner, 1947; Lotz, 1974). However, the absence of any specific side chain leads to a highly solvated polypeptide backbone that has strong effects on the energetics of the unfolded state (Avbelj and Baldwin, 2002). Hence, the properties of glycine residues that determine how readily such a structure is adopted may not readily compare with those of chiral residues.

Implications for aggregation reactions involved in conformational diseases

The formation of amyloid structures is the underlying molecular event of a range of human diseases (Sunde and Blake, 1998; Dobson 2001). Our proposals concerning the question of how amyloid formation can be explained from the chemical and structural properties of the polypeptide chain therefore address the common molecular basis for these different pathological conditions. According to these ideas, there are two fundamental modes in which polypeptide chains can be organized into a stable conformation. One of them, the amyloid structure, reflects the common polymer properties of polypeptide chains, whereas the other state (the globular protein conformation) is specific for each polypeptide chain. The latter form, however, is the one that generally has been utilized by nature for functional roles in living organisms. Amyloidoses therefore represent pathological conditions that can arise if a natural polypeptide chain adopts this generic polymer structure rather than the specific (protein) conformation that is encoded in its sequence.

Many apparently unrelated observations concerning the formation of specific pathological fibrils can readily be seen to represent specific cases of a more general structural principle. For example, amyloid formation has been associated with unstable globular protein conformations (Kelly et al., 1996; Dobson, 2001; Fändrich et al., 2001), hydrophobicity (Rochet and Lansbury, 2000; Chiti et al., 2002), enrichment in glutamine or asparagine residues (Perutz et al., 1994; DePace et al., 1998) or the absence of the specific ionic interactions characteristic of edge strands (Richardson and Richardson, 2002). It is particularly interesting that an increasing number of different PAAs has been described to give rise to disease or pathological fibrils. Poly-L-glutamine was the first PAA to be identified in this context. It was found that genetic mutations within the open reading frame of cellular proteins can lead to aberrant poly-L-glutamine stretches, intranuclear fibrous aggregates and diseases such as Huntington's (Perutz et al., 1994). The formation of these aggregates has been explained previously on the basis of the specific polarity of glutamine side chains (Perutz et al., 1994). However, poly-L-alanine extensions have also been observed to

cause disease (oculopharyngeal muscle dystrophy) and to be associated with pathological fibrils (Calado et al., 2000). Moreover, there is the recent report of a disorder termed 'Huntington disease-like 2' that depends on abnormal poly-L-leucine repeats (Holmes et al., 2001).

Whereas the wild-type sequences of natural polypeptide chains are likely to be selected in order to suppress the formation of generic polypeptide states by means of the inverse sequence effect described here, specific cases have been documented in which amyloid structures play a functional role in vivo or increase the evolutionary fitness of the affected organism. Examples include the yeast prions that represent the inheritance mechanism of a specific phenotype [PSI+] (True and Lindquist, 2000) or the 'curli fibrils' of Escherichia coli (Chapman et al., 2002). Downstream events can therefore determine the specific effect that a particular polypeptide aggregate will produce within its cellular environment. We believe, however, that the concepts discussed here concerning the molecular basis of amyloid formation can provide the key to understand the underlying structural origins of these diseases and, indeed, of other phenotypes that arise from aggregated polypeptides.

Materials and methods

Polyamino acids and amino acid hydrolysis

PE (74.4 kDa), PT (7.6 kDa) and PK (77.3 kDa) were purchased from Sigma (Gillingham, UK). PT and PK were dialysed and lyophilized before use, whereas PE was used without further purification. To test for covalent modifications, PAA aliquots (20 μg) were hydrolysed in 6 M HCl at 150°C, dried and re-dissolved in 2:1 methanol:diisopropylethylamine (DIEA). After a further drying step, the material was derivatized in 15 μl of a 7:2:2 mixture of methanol/DIEA/(5% phenylisothiocyanate in heptane). Reversed phase analyses were carried out at 254 nm using a Vydac 218TP54 column and acetonitrile gradients (0.1% TFA). These results were confirmed independently by an amino acid analysis carried out in the laboratory of L.Packman (Department of Biochemistry, University of Cambridge).

Electron microscopy

For negative staining, specimens were prepared on carbon-coated mica sheets and stained with 2% uranyl acetate solution using the floating carbon method. A freshly cleaved mica sheet was coated with carbon. Aliquots of the sample solution were diluted (typically 10-fold in buffer or pure water), inserted between the carbon layer and the mica and left for 3 min to enable binding to the carbon film. The mica was then transferred to the top of an uranyl acetate droplet (50 μl) so that the carbon film would fully dissociate from the mica and float on the uranyl acetate. Using a 400 square mesh grid, the carbon film was removed immediately from the staining solution and air dried. The samples were analysed with a JEM 1010 transmission electron microscope at 80 kV excitation voltage.

Circular dichroism and Fourier transform infrared spectroscopy

The CD measurements were carried out in a Jasco J-720 spectropolarimeter (Great Dunmow, UK). Solutions of 0.1 mg/ml were exposed to the respective guanidine hydrochloride concentration for 10 h before the analysis. The guanidine concentration in each sample was determined by refractometry. FTIR samples were prepared in D_2O, and the pD value was adjusted using DCl or NaOD (Sigma). Quoted pD values were not corrected for isotope effects. Sample aliquots were placed between two CaF_2 windows separated by a 50 μm spacer. Spectra were recorded at room temperature in a Bio-Rad FTS 175C FT-IR spectrometer equipped with an MCT detector cooled with liquid nitrogen. The sample compartment was purged thoroughly with dry nitrogen, and all spectra shown represent the average of 256 acquisitions.

X-ray diffraction

Sample solutions were dried onto glass slides. The resulting films were lifted off and mounted with their planes parallel to the beam. X-ray images were obtained by using an 18 cm Mar imaging plate detector (MarResearch, Norderstedt, Germany) mounted on a Rigaku RU200 rotating anode source of Cu Kα (1.5418 Å). The sample to detector distance was 100 mm and the image files were displayed using IPDISP software from the CCP4 package (CCP4, 1994).

References

Abkevich,V.I., Gutin,A.M. and Shakhnovich,E.I. (1998) Theory of kinetic partitioning in protein folding with possible applications to prions. *Proteins Struct. Funct. Genet.*, 31, 335–344.

Anfinsen,C.B. (1973) Principles that govern the folding of protein chains. *Science*, 181, 223–230.

Arnott,S., Dover,S.D. and Elliott,A. (1967) Structure of β-poly-L-alanine: refined atomic co-ordinates for an anti-parallel β-pleated sheet. *J. Mol. Biol.*, 30, 201–208.

Avbelj,F. and Baldwin,R.L. (2002) Role of backbone solvation in determining thermodynamic β propensities of the amino acids. *Proc. Natl Acad. Sci. USA*, 99, 1309–1313.

Baker,D. (2000) A surprising simplicity to protein folding. *Nature*, 405, 39–42.

Baskakov,I.V., Legname,G., Prusiner,S.B. and Cohen,F.E. (2000) Folding of prion protein to its native α-helical conformation is under kinetic control. *J. Biol. Chem.*, 276, 19687–19690.

Blondelle,S.E., Forood,B., Houghten,R.A. and Pérez-Payá,E. (1997) Polyalanine-based peptides as models for the self-associated β-pleated-sheet complexes. *Biochemistry*, 36, 8393–8400.

Bunn,C.W. and Garner,E.V. (1947) The crystal structure of two polyamides ('nylons'). *Proc. R. Soc. Lond. Ser. A*, 189, 39–68.

Calado,A., Tome,F.M.S., Brais,B., Rouleau,G.A., Kühn,U., Wahle,E. and Carmo-Fonseca,M. (2000) Nuclear inclusions in oculopharyngeal muscular dystrophy of poly(A)binding protein 2 aggregates which sequester poly(A) RNA. *Hum. Mol. Genet.*, 9, 2321–2328.

CCP4(1994) The CCP4 suite: programs for protein crystallography. *Acta Crystallogr. D*, 50, 760–763.

Chapman,M.R., Robinson,L.S., Pinkner,J.S., Roth,R., Heuser,J., Hammar,M., Normark,S. and Hultgren,S.J. (2002) Role of *Escherichia coli* curli operons in directing amyloid fiber formation. *Science*, 295, 851–855.

Chiti,F., Webster,P., Taddei,N., Clark,A., Stefani,M., Ramponi,G. and Dobson,C.M. (1999) Designing conditions for *in vitro* formation of amyloid protofilaments and fibrils. *Proc. Natl Acad. Sci. USA*, 96, 3590–3594.

Chiti,F., Taddei,N., Baroni,F., Capanni,C., Stefani,M., Ramponi,G. and Dobson,C.M. (2002) Kinetic partitioning of protein folding and aggregation. *Nat. Struct. Biol.*, 9, 137–143

Creighton,T.E. (1993) *Proteins: Structure and Molecular Properties*, 2nd edn. W.H. Freeman and Company, New York, NY.

DePace,A.H., Santoso,A., Hillner,P. and Weissman,J.C. (1998) A critical role for amino-terminal glutamine/asparagine repeats in the formation and propagation of a yeast prion. *Cell*, 93, 1241–1252.

Dill,K.A., Bromberg,S., Yue,K., Fiebig,K.M., Yee,D.P., Thomas,P.D. and Chan,H.S. (1995) Principles of protein folding—a perspective from simple exact models. *Protein Sci.*, 4, 561–602.

Dobson,C.M. (1999) Protein misfolding, evolution and disease. *Trends Biochem. Sci.*, 24, 329–332.

Dobson,C.M. (2001) The structural basis of protein folding and its links with human disease. *Philos. Trans. R. Soc. Lond. Ser. B.*, 356, 133–145.

Dobson,C.M., Sali,A. and Karplus,M. (1998) Protein folding: a perspective from theory and experiment. *Angew. Chem. (Int. Ed.)*, 37, 868–893.

Fändrich,M., Fletcher,M.A. and Dobson,C.M. (2001) Amyloid fibrils from muscle myoglobin. *Nature*, 410, 165–166.

Glenner,G.G., Eanes,E.D. and Page,D.L. (1972) The relation of the properties of Congo red-stained amyloid fibrils to the β-conformation. *J. Histochem. Cytochem.*, 20, 821–826.

Glenner,G.G., Eanes,E.D., Bladen,H.A., Linke,R.P. and Termine,J.D. (1974) β-Pleated sheet fibrils: a comparison of native amyloid with synthetic protein fibrils. *J. Histochem. Cytochem.*, 22, 1141–1158.

Greenfield,N. and Fasman,G.D. (1969) Computed circular dichroism spectra for the evaluation of protein conformation. *Biochemistry*, 8, 4108–4116.

Groß,M., Wilkins,D.K., Pitkeathly,M.C., Chung,E.W., Higham,C., Clark,A. and Dobson,C.M. (1999) Formation of amyloid fibrils by peptides derived from the bacterial cold shock protein CspB. *Protein Sci.*, 8, 1350–1357.

Holmes,S.E. *et al.* (2001) A repeat expansion in the gene encoding junctophilin-3 is associated with Huntington disease-like 2. *Nat. Genet.*, 29, 377–378.

Inouye,H., Fraser,P.E. and Kirschner,D.A. (1993) Structure of β-crystallite assemblies formed by Alzheimer β-amyloid protein analogues: analysis by X-ray diffraction. *Biophys. J.*, 64, 502–519.

Inouye,H., Bond,J., Baldwin,M.A., Ball,H.L., Prusiner,S.A. and Kirschner,D.A. (2000) Structural changes in a hydrophobic domain of the prion protein induced by hydration and by Ala→Val and Pro→Leu substitutions. *J. Mol. Biol.*, 300, 1283–1296.

Keith,H.D., Padden,F.J.,Jr and Giannoni,G. (1969) Crystal structures of β-poly-L-glutamic acid and its alkaline earth salts. *J. Mol. Biol.*, 43, 423–438.

Kelly,J.W. (1996) Alternative conformations of amyloidogenic proteins govern their behavior. *Curr. Opin. Struct. Biol.*, 6, 11–17.

Kirschner,D.A., Elliott-Bryant,R., Szumowski,K.E., Gonnerman,W.A., Kindy,M.S., Sipe,J.D. and Cathcart,E.S. (1998) *In vitro* amyloid fibril formation by synthetic peptides corresponding to the amino terminus of apoSAA isoforms from amyloid-susceptible and amyloid-resistant mice. *J. Struct. Biol.*, 124, 88–98.

Komoto,T., Kim,K.Y., Oya,M. and Kawai,T. (1974) Crystallization of polypeptides in the course of polymerisation, 5. Effect of the steric hindrance on the crystal growth by the side chains. *Makromol. Chem.*, 175, 283–299.

Lotz,B. (1974) Crystal structure of polyglycine I. *J. Mol. Biol.*, 87, 169–180.

Luckey,M., Hernandez,J.F., Arlaud,G., Forsyth,V.T., Ruigrok,R.W.H. and Mitraki,A. (2000) A peptide from the adenovirus fibre shaft forms amyloid-type fibrils. *FEBS Lett.*, 468, 23–27.

Malinchik,S.B., Inouye,H., Szumowski,K.E. and Kirschner,D.A. (1998) Structural analysis of Alzheimer's β(1–40) amyloid: protofilament assembly of tubular fibrils. *Biophys. J.*, 74, 537–545.

Moriarty,D.F. and Raleigh,D.P. (1999) Effects of sequential proline substitutions on amyloid formation by human amylin$_{20-29}$. *Biochemistry*, 38, 1811–1818.

Nguyen,J.T., Inouye,H., Baldwin,M.A., Fletterick,R.J., Cohen,F.E., Prusiner,S.B. and Kirschner,D.A. (1995) X-ray diffraction of scrapie prion rods and PrP peptides. *J. Mol. Biol.*, 252, 412–422.

Padden,F.J.,Jr, Keith,H.D. and Giannoni,G. (1969) Single crystals of poly-L-lysine. *Biopolymers*, 7, 793–804.

Perutz,M.F., Johnson,T., Suzuki,M. and Finch,J.T. (1994) Glutamine repeats as polar zippers: their possible role in inherited neurodegenerative diseases. *Proc. Natl Acad. Sci. USA*, 91, 5355–5358.

Perutz,M.F., Pope,B.J., Owen,D., Wanker,E.E. and Scherzinger,E. (2002) Aggregation of proteins with expanded glutamine and alanine repeats of the glutamine-rich and asparagine-rich domains of Sup35 and of the amyloid β-peptide of amyloid plaques. *Proc. Natl Acad. Sci. USA*, 99, 5596–5600.

Prusiner,S.B. (1998) Prions. *Proc. Natl Acad. Sci. USA*, 95, 13363–13383.

Richardson,J.S. and Richardson,D.C. (2002) Natural β-sheet proteins use negative design to avoid edge-to-edge aggregation. *Proc. Natl Acad. Sci. USA*, 99, 2754–2759.

Rochet,J.-C. and Lansbury,P.T.,Jr (2000) Amyloid fibrillogenesis: themes and variations. *Curr. Opin. Struct. Biol.*, 10, 60–68.

Santoro,M.M. and Bolen,D.W. (1988) Unfolding free energy changes determined by the linear extrapolation method. 1. Unfolding of phenylmethanesulfonyl α-chymotrypsin using different denaturants. *Biochemistry*, 27, 8063–8068.

Serpell,L.C., Blake,C.C.F. and Fraser,P.E. (2000) Molecular structure of a fibrillar Alzheimer's Aβ fragment. *Biochemistry*, 39, 13269–13275.

Sunde,M. and Blake,C.C.F. (1998) From the globular to the fibrous state: protein structure and structural conversion in amyloid formation. *Q. Rev. Biophys.*, **31**, 1–39.

Sunde,M., Serpell,L.C., Bartlam,M., Fraser,P.E., Pepys,M.B. and Blake,C.C.F. (1997) Common core structure of amyloid fibrils by synchrotron X-ray diffraction. *J. Mol. Biol.*, **273**, 729–739.

Symmons,M.F., Buchanan,S.G.S.C., Clarke,D.T., Jones,G. and Gay,N.J. (1997) X-ray diffraction and far-UV CD studies of filaments formed by a leucine-rich repeat peptide: structural similarity to the amyloid fibrils of prions and Alzheimer's disease β-protein. *FEBS Lett.*, **412**, 397–403.

True,H.L. and Lindquist,S.L. (2000) A yeast prion provides a mechanism for genetic variation and phenotypic diversity. *Nature*, **407**, 477–483.

Villegas,V., Zurdo,J., Filimonov,V.V., Avilés,F.C., Dobson,C.M. and Serrano,L. (2000) Protein engineering as a strategy to avoid formation of amyloid fibrils. *Protein Sci.*, **9**, 1700–1708.

Weaver,L., Stagsted,J., Behnke,O., Matthews,B.W. and Olsson,L. (1996) β-Sheet models for the ordered filamentous structure formed by a peptide that enhances the action of insulin. *J. Struct. Biol.*, **117**, 165–172.

West,M.W., Wang,W., Patterson,J., Mancias,J.D., Beasley,J.R. and Hecht,M.H. (1999) *De novo* amyloid proteins from designed combinatorial libraries. *Proc. Natl Acad. Sci. USA*, **96**, 11211–11216.

Wigley,W.C., Corboy,M.J., Cutler,T.D., Thibodeau,P.H., Oldan,J., Lee,M.G., Rizo,J., Hunt,J.F. and Thomas,P.J. (2002) A protein sequence that can encode native structure by disfavouring alternate conformations. *Nat. Struct. Biol.*, **9**, 381–388.

Zurdo,J., Guijarro,J.I., Jimenez,J., Saibil,H.R. and Dobson,C.M. (2001) Dependence on solution conditions of aggregation and amyloid formation by an SH3 domain. *J. Mol. Biol.*, **311**, 325–340.